25228

National Library of Canada
Bibliothèque nationale du Canada

CANADIAN THESES ON MICROFICHE

THÈSES CANADIENNES SUR MICROFICHE

NAME OF AUTHOR/*NOM DE L'AUTEUR* BRIAN BARRY NAROD

TITLE OF THESIS/*TITRE DE LA THÈSE* ULTRA HIGH FREQUENCY RADIO ECHO SOUNDING OF GLACIERS

UNIVERSITY/*UNIVERSITÉ* OF BRITISH COLUMBIA

DEGREE FOR WHICH THESIS WAS PRESENTED/ *GRADE POUR LEQUEL CETTE THÈSE FUT PRÉSENTÉE* M. Sc.

YEAR THIS DEGREE CONFERRED/*ANNÉE D'OBTENTION DE CE GRADE* 1975

NAME OF SUPERVISOR/*NOM DU DIRECTEUR DE THÈSE* G. K. C. CLARKE

Permission is hereby granted to the NATIONAL LIBRARY OF CANADA to microfilm this thesis and to lend or sell copies of the film.

The author reserves other publication rights, and neither the thesis nor extensive extracts from it may be printed or otherwise reproduced without the author's written permission.

L'autorisation est, par la présente, accordée à la BIBLIOTHÈQUE NATIONALE DU CANADA de microfilmer cette thèse et de prêter ou de vendre des exemplaires du film.

L'auteur se réserve les autres droits de publication; ni la thèse ni de longs extraits de celle-ci ne doivent être imprimés ou autrement reproduits sans l'autorisation écrite de l'auteur.

DATED/*DATÉ* May 1-75 SIGNED/*SIGNÉ* B Barry Narod

PERMANENT ADDRESS/*RÉSIDENCE FIXE* #201 2234 W 1st Ave
VANCOUVER, B.C.

NL-91 (3-74)

ULTRA HIGH FREQUENCY RADIO ECHO SOUNDING OF GLACIERS

by

B. Barry Narod

B.Sc., University of British Columbia, 1970

A THESIS SUBMITTED IN PARTIAL FULFILMENT OF
THE REQUIREMENTS FOR THE DEGREE OF
MASTER OF SCIENCE

in the Department
of
Geophysics and Astronomy

We accept this thesis as conforming to the
required standard

Garry Clarke
....

R D Russell
....

....

The University of British Columbia
April 1975

© B. Barry Narod 1976

In presenting this thesis in partial fulfilment of the requirements for an advanced degree at the University of British Columbia, I agree that the Library shall make it freely available for reference and study. I further agree that permission for extensive copying of this thesis for scholarly purposes may be granted by the Head of my Department or by his representatives. It is understood that copying or publication of this thesis for financial gain shall not be allowed without my written permission.

B. Barry Narod

Department of Geophysics & Astronomy

The University of British Columbia
2075 Wesbrook Place
Vancouver, Canada
V6T 1W5

Date May 1 '75

DE-6 BP 74-4456

ABSTRACT

For determining the thickness of ice, radio echo sounding of glaciers is well established as a technique for rapid gathering of data. However it has become evident that radio echo sounder parameters must be tailored to meet specific requirements in order to achieve best results.

In particular rapid sounding of temperate, alpine glaciers and larger polar valley glaciers could be surveyed by a radio echo sounder having a very short pulse, very wide band response and narrow beam antenna. Such requirements can be fulfilled by Ultra High Frequency (300 MHz - 3 GHz) radio echo sounders, improved performance being achieved at the expense of decreased maximum range.

This thesis, after considering previous attempts at radio echo sounding of glaciers, with respect to surveying valley and temperate glaciers, proposes and details a UHF radio echo sounder operating at 840 MHz. Conventional performance is predicted, and some new experiments, possible because of the short wavelength, are proposed.

Appended to the thesis is a review and discussion of problems associated with the use of thermistors as thermometers in snow or ice. A procedure is described for optimizing the techniques of thermistor selection and use.

TABLE OF CONTENTS

Abstract I

List Of Tables Iv

List Of Figures V

Acknowledgements Vi

Chapter 1: Introduction 1

  1.1 Background 1

  1.2 Dielectric Properties Of Ice 4

Chapter 2: System Design 6

  2.1 General Description 6

  2.2 Selection Of The Carrier Frequency 7

  2.3 System Performance & Range 10

  2.4 Antenna Design 12

Chapter 3: Circuit Design 15

  3.1 Transmitter Circuit 17

  3.2 Receiver/pulse Generator Circuit 18

  3.3 Display And Recorder 21

Chapter 4: System Capabilities 25

  4.1 System Performance 25

  4.2 Maximum Range And Resolution 26

  4.3 Reflectivity Of Layers Within A Glacier 28

  4.4 Polarization 29

  4.5 Conclusion 34

Bibliography 36

Appendix 45

1 Introduction 46

2 Thermistor Characteristics 48

3 Bridges And Bridge Power Supply 52

4 Transmission Line Effects 61

5 Evaluation Of Available Systems (dsm.s) 62

Conclusion 64

Bibliography 67

LIST OF TABLES

Table 2.1: Radar Parameters 7

Table 2.2: System Performance 10

Table 1: Digital Multimeters 63

Table 2: Digital Multimeter Errors 64

LIST OF FIGURES

Figure 2.1 13
Figure 3.1: Radar Interconnection Diagram 16
Figure 3.2: Transmitter Block Diagram 17
Figure 3.3: Receiver Block Diagram 19
Figure 3.4: Intensity Modulation Recording Block Diagram .23
Figure 3.5: Digitizer Block Diagram 24
Figure 1: Generalized Bridge 47
Figure 2: Bridge Configurations 54
Figure 3: Digital Multimeter Errors 64

ACKNOWLEDGEMENTS

I wish to thank my supervisor, Dr. Garry Clarke, for his patience and guidance during the course of this work. I would also like to thank Dr. Clarke, Dr. R. D. Russell, the Department of Geophysics and Astronomy, and the Department of Physics for financial support I received while I was completing this thesis.

I am very grateful to Dr. Ron Goodman of Calgary for his invaluable assistance and advice while development of the radio echo sounder progressed.

I wish to acknowledge the services of the University's Computing Center, which supported this typescript; and the numerous manufacturers who participated in the development of the radio echo sounder. I thank the Department of Geophysics and Astronomy for providing laboratory facilities for this project.

I thank all of my friends among the faculty, staff and students of the Department, especially Mr. Peter Michelow, for all their contributions to this project.

Finally, and especially, I wish to thank the National Research Council of Canada which financed the development of both the UHF radio echo sounder and the thermistor resistance bridge. The radio echo sounder was financed by grant A3479 from the National Research Council to Dr. Clarke. The resistance bridge was financed by grant A4327 from the

National Research Council of Canada also to Dr. Clarke.

CHAPTER 1: INTRODUCTION

1.1 BACKGROUND

Radio echo sounding of ice was "successful" as early as 1946 when aircraft pilots using pulsed radar altimeters over Antarctic ice reported possible fatal errors in radar interpretation. In 1955 440 MHz pulsed radar altimeters attempted the first intentional vertical transmission through ice on the 800 ft. thick Ross Ice Shelf. A lack of results induced attempts in 1958 to probe 500 ft. thick ice at Wilkes Station. Strong echoes combined with seismic information provided information about the propagation velocity of electromagnetic radiation in ice. Further work in Greenland confirmed the dielectric constant value in ice of 3.2 (von Hippel, 1954). In 1960 tests were made of altimeters operating at 110, 220, 440 and 4300 MHz. These showed that the lowest frequencies were most suited to sounding of thick ice. A summary was reported by Waite and Schmidt (1962).

In 1963, the British Antarctic Survey operated the 35 MHz SPRI Mk I apparatus, the first radar system designed specifically for the use of sounding ice sheets. The SPRI Mk I sounder had a 40 W r.m.s. transmitter pulse power, a -93 dBm receiver sensitivity, a 10 MHz bandwidth and monopole antennae (Evans, 1963a). Further tests by the Scott Polar

Research Institute (SPRI) and the U. S. Army Electronics Laboratory (USAEL) determined that signal attenuation was reduced at lower frequencies (Evans, 1963b).

During the following field season the Ninth Soviet Antarctic Expedition (Bogorodskiy, Rudakov, Tyul'pin, 1965) operated a type-1M4 radar apparatus, with a carrier frequency of 213 MHz, and a pulse power of 80 Kw r.m.s. Strong echoes were obtained from depths up to 900 m. The project terminated with the loss of the apparatus and the driver into a crevasse.

The next three years saw expanded use of the SPRI Mk II sounder (500 w pulse power, otherwise same as Mk I) and the SCR 718 radio altimeter (440 MHz), including airborne surveying in Canada, Greenland and Antarctica (Evans, 1966).

The SPRI operated a SPRI Mk IV sounder from an aircraft during the 1969-70 field season. Flight lines are in Evans and Smith, (1971). The following year the SPRI operated a modified SPRI Mk IV apparatus (modified to 60 MHz) from an aircraft. Butterfly plan multi-wire dipole antennae were used to maintain a large bandwidth. A maximum ice thickness of 4450 m was recorded (Evans, Drewry, Robin, 1972).

In 1973 Davis, Halliday and Miller reported a Cambridge expedition attempt to sound the Roslin Gletscher in Stauning Alper, East Greenland, using a modified SCR 718 radio altimeter with a 45° corner reflector antenna. Up to this time all radio sounding had been with systems equipped with monopole, dipole or two element Yagi antennae. For frequencies below 300 MHz high gain antennae would be prohibitively large. Sounding in ice sheets, however, could be improved by using higher power transmitters. Returned power that arrived later than the initial bottom bounce did not affect the accuracy of the record. In valley glaciers, wall echoes could obscure or be mistaken for bottom echoes. Davis et al (1973) recognized that in order to achieve consistent results radiated and received power must be restricted to a narrow beam. Using an antenna with 8 dB forward gain they recorded echoes up to 350 m.

In 1972, in a continuing project, the Department of Energy Mines and Resources, Canada, made soundings on the Athabasca Glacier, Alberta, Canada, with a UHF apparatus developed by R. Goodman. The unit featured a 620 MHz carrier frequency, 3 Kw pulse power and a very high gain corner reflector antenna. Results were generally negative, but very fine interglacier structure was detected. The following year the unit was operated on the Trapridge and Rusty Glaciers, surging glaciers in the Yukon Territory, Canada, with total success (Clarke & Goodman, 1975; Goodman et al, 1975).

In 1974, using a transmitter developed by the Stanford Research Institute, Watts, Meier et al (1974) made soundings on the South Cascade Glacier, Washington U.S.A. and the Columbia Glacier, Alaska, U.S.A. The apparatus featured a monopulse signal with 1-5 MHz carrier frequency and 100 ns pulse length. Successful soundings were made up to 1200 m in temperate ice (Meier & Watts, private communication). Its chief disadvantage was in its antennae configuration. It was necessary to use butterfly half wave dipoles spread on the glacier surface. The transmitter and receiver antennae were separated by 50 m. This configuration precludes continuous profiling due to its size and its method of deployment.

Radio echo sounding has been established as a practical method for obtaining ice thicknesses, with reasonable reliability. Sounding in large polar ice masses is most satisfactory at low frequencies, the lower limit being determined by antenna size and communication interference. Large temperate ice masses could be sounded with low frequency monopole sounders. However sounding in smaller valley and alpine glaciers, in particular temperate or partially temperate glaciers, could be successfully studied with UHF sounders. These sounders have very narrow antennae beams, very fast risetimes and short pulse lengths. They will be the most practical system for continuous profiling over these glaciers.

1.2 DIELECTRIC PROPERTIES OF ICE

1.2.1 PERMITTIVITY

Pure ice has a relatively high static permittivity (approximately 100) (Evans, 1965) and a long relaxation time

(0.1 ms) due to its polar molecules. At radio frequencies of the order of 1 MHz the effects of the relaxation spectrum, and its corresponding effect with temperature on the relative permittivity have virtually vanished. Numerous programs have detemined that above 1 MHz the relative permittivity of ice is 3.2±0.2 (Auty & Cole, 1952; Cumming, 1952; von Hippel, 1954). It is virtually independent of temperature, and in temperate ice it is suspected that water content is insufficient to cause large variations (Evans, 1965).

1.2.2 LOSS TANGENT

In 0°C ice below 300 MHz, $f\tan\delta$ is virtually constant, and in spite of the lack of effect on permittivity, power losses are due primarily to the relaxation spectrum. Above 300 MHz infrared absorption becomes evident. At reduced temperatures, the infrared absorption, which is relatively temperature insensitive, is evident at lower frequencies. Residual absorption from the relaxation spectrum decreases with lower temperatures (Evans, 1965).

In temperate ice, water content can have widely varying effects on the loss tangent. This is due in part to the wide relaxation spectrum of water, but probably D.C. conductivity of water and scattering by water inclusions provide the greatest losses (Evans, 1965; Smith & Evans, 1972).

CHAPTER 2: SYSTEM DESIGN

2.1 GENERAL DESCRIPTION

In designing a radio echo sounder for sounding in valley glaciers one has basically five parameters to work with: carrier frequency, bandwidth, pulse length, antenna pattern and peak transmitter power. Echo risetime at the receiver is determined by transmitter, receiver and antenna bandwidth and by the antenna pattern. Maximum range is determined by the peak transmitter power, the carrier frequency, and the antenna pattern. Resolution is affected by pulse length, system bandwidth and antenna pattern

The parameters for a system designed at the University of British Columbia are listed in table 2.1. The carrier frequency is 840 MHz, the bandwidth is 40 MHz, the pulse length is 70 ns, the antenna gain is 19 dB and the peak r.m.s. transmitter power is 4.1 Kw.

2.2 SELECTION OF THE CARRIER FREQUENCY

The decision to operate at 840 MHz can be divided into two steps. First, the decision to operate within the U.H.F. T.V. band. Secondly, what frequency within the band to use.

TRANSMITTER PARAMETERS		
	Operating frequency	840 MHz
	Bandwidth	35 MHz
	Pulse length	70 ns
	Rise time	18 ns
	Fall time	28 ns
	Peak power	4.1 Kw (66 dBm)
	Repetition rate	25 KHz
ANTENNA CONFIGURATION		90° dual dipole corner reflector
	Gain	19dB over isotropic
	Front/side ratio	60 dB
	VSWR	≤ 1.5
RECEIVER PARAMETERS		
	Bandwidth	40 MHz
	Dynamic range	97 dB
	Minimum sensitivity	-82 dBm
SYSTEM PERFORMANCE		
	Single antenna	> 95 dB
	Dual antenna	138 dB

TABLE 2.1: RADAR PARAMETERS

The prime factor in choosing a high frequency is the constraint that the first use of the system will be to sound small icecaps and valley glaciers of the Canadian Arctic and Northwest, where valley wall echoes necessitate a high gain antenna. VHF or lower frequencies cannot be operated with a high gain antenna which would be conveniently small for either aerial or surface use. The useful frequency range is limited to 300 MHz or higher (Davis, 1973).

Once the decision has been made to operate within the useful UHF range (300MHz - 1GHz) a single frequency must be selected.

In sounding -20°C ice at these frequencies ftan δ increases as the second power of the frequency (Walford, 1968; Bleaney & Bleaney, 1957). This is countered by the antenna gain, in that for a given aperture size gain also goes up as the second power of the frequency, and the effects cancel. The advantage of using a higher frequency lies in the narrower beamwidth available for a given aperture size. The beam will illuminate a smaller area of the glacier bed, hence clearer echoes will be achieved.

As the temperature increases the variation of ftan δ with frequency decreases so that at 0°C ftan δ, or attenuation per unit length is effectively constant ($0.057 dBm^{-1}$: Smith & Evans, 1972) hence the advantage of going to a higher frequency due to having a greater gain for a given aperture is real. The two way gain increases as the fourth power of the frequency whereas transmission losses decrease only as the second power. The advantage of the narrower beamwidth still applies, especially considering that the beam will illuminate fewer scattering objects whose range is close to the range of the bedrock (Davis, 1973). Davis (1973) also suggests that scattered power may actually tend to decrease with these higher frequencies, although evidence for this is limited.

The final decision to use 840 MHz rather than any nearby frequency (either higher or lower) is economic. 840 MHz ± 20 MHz lies within a common carrier landbased mobile, and interim UHF TV band for which hardware is more easily available. Due to its dual use, this frequency has been set as a break point in transmitter design; any lower frequency would require a larger, more expensive cavity amplifier (R.L. Sepulveda, Microwave Control Co., private communication).

2.2.1 TRANSMITTER DESIGN

At the carrier frequency selected it is more stable to employ a crystal frequency generator rather than use an L-C tank to produce the frequency, as is the case with more conventional systems such as the SPRI MK II.

The transmitter derives its frequency from a 120 MHz crystal oscillator, fed into a x7 multiplier. Two stages of amplification and modulation lead the signal to a cavity triode R.F. power amplifier. Here some of the advantages of the crystal generated frequency become apparent. It is much easier to detune the characteristicly high Q of a cavity amplifier, giving the efficient result of having all of the transmitted power within the receiver bandwidth.

2.2.2 ANTENNA & TRANSMIT/RECEIVE SWITCH

A corner reflector antenna was selected for the prototype configuration. With a two colinear dipole driven element the antenna should have sufficiently high gain and narrow beam width to yield strong echoes with short fading patterns. Concurrently the 90° side lobes should be sufficiently low that valley wall echoes will not obscure bottom echoes when the apparatus is operated at the ice surface.

A circulator is used as a passive transmit/receive switch when the system is operated with a single antenna.

2.2.3 RECEIVER AND RECORDER

The receiver has a logarithmic intermediate frequency (I.F.) amplifier as its primary component. Initially a photographic X-Y or intensity-modulated recording will be used. In the future it is hoped to be able to record the signals digitally onto magnetic tapes.

2.3 SYSTEM PERFORMANCE & RANGE

The smaller more efficient cavities available at this frequency yield higher peak power, hence greater system performance. Important parameters are listed in Table 2.2.

If we assume dielectric losses D of 0.057dBm^{-1} and a bedrock reflection coefficient R of -20 dB (Robin, Evans, Bailey, 1969; Harrison, 1972) an antenna gain G of 19 dB and a system performance of 138 dB then the maximum range is determined by

$$\frac{P_{received}}{P_{transmitted}} = \frac{G^2\lambda^2R}{64\pi^2r^2}\,10^{-0.2Dr} \qquad (1)$$

Peak power	66 dBm
Receiver sensitivity	--90 dBm
Mixer conversion loss	-8 dB
Maximum system performance	138 dB
Linear system performance	118 dB[1]

[1] Receiver is linear down to -70 dBm.

TABLE 2.2: SYSTEM PERFORMANCE

The maximum range r is then 700 m which should be ample for sounding many valley glaciers.

According to Davis (1973) a criterion for successful sounding of temperate glaciers is

$$\frac{P_{r(plane)}}{P_{r(scattered)}} = \frac{R}{C}\left(\frac{G-1}{l_m}\right) > 1 \qquad (2)$$

where R is the bedrock reflectivity, assumed to be -20 dB; C is the scattering coefficient, calculated to be 0.01 m^{-1} (based on Davis' (1973) analysis of the DEMR sounder operating at 620 MHz); G is the antenna gain, set at 19 dB and l is the pulse length in ice. In our case

$$\frac{R}{C}\left(\frac{G-1}{l_m}\right) = \frac{0.01}{0.01/m}\left(\frac{80-1}{11m}\right) = 7 \qquad (3)$$

hence our system should be successful at sounding temperate glaciers.

2.4 ANTENNA DESIGN

There are numerous styles of antennae which can provide large bandwidth and high gain at the frequencies discussed here. Some are capable of very great broadbanding. The Yagi, paraboloid, helical and broadside array are some. However, in selecting an antenna to sound valley glaciers, forward gain is not the only constraint. Equally important is the 90° side lobe level, or the "front to side" ratio.

In a valley, the dip of the valley walls rarely exceeds 45° [Fig. 2.1]. If we model a glacier as filling approximately a paraboloidal valley it follows that over a large range of distances from the valley wall, L, the travel time for the transmitted pulse to reach the valley wall closely matches the time for that pulse to reach the bed, at height H below the ice surface (using a velocity in ice of 176 m/ sec). Since the surface wave is not noticably attenuated, in a large glacier the valley wall echo may easily obscure or be confused with the bottom echo.

For example the paraboloidal reflector antenna has a front to side ratio of 30 dB. With 0.05 dBm^{-1} attenuation in ice the bottom echo will be the same strength as the wall echo

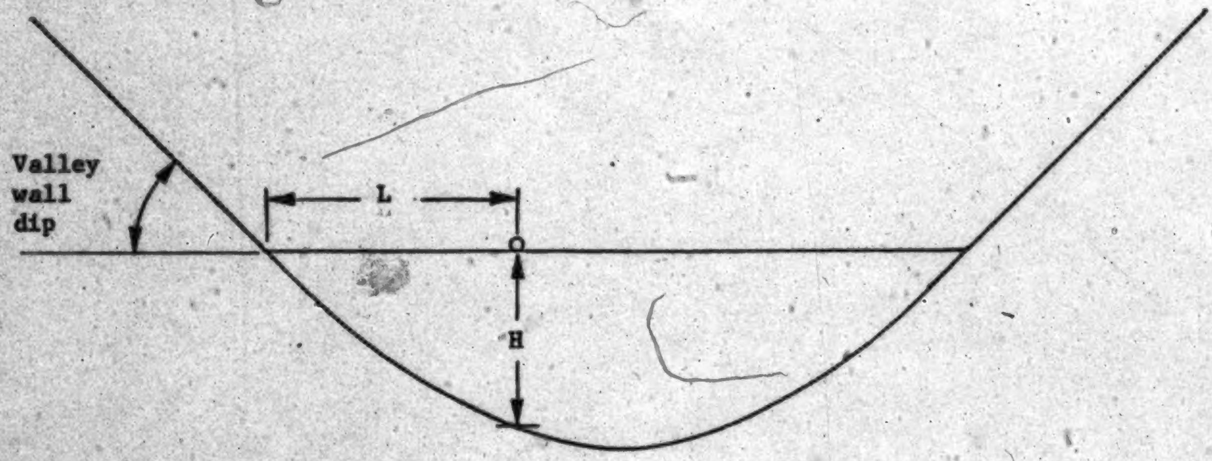
Valley
wall
dip
L
H

FIGURE 2.1

after only 600 m of two way travel. In temperate ice this maximum range decreases rapidly.

Ideally the front to side ratio should not be greater than one half the system performance in order to have power returned from the walls obscured in system noise. It is possible to achieve a front to side ratio of 60 dB by using a corner reflector. This will reduce system performance to 120 dB when operated in such a valley. Aperture synthesis may improve the front to side ratio still further, though this technique is difficult and necessarily very slow.

CHAPTER 3: CIRCUIT DESIGN

The radio echo sounder consists of five units (not including power supply) connected in the field only during use. They are the transmitter, circulator, antenna, receiver/pulse generator, and display. The assembly is depicted in Figure 3.1.

3.1 TRANSMITTER CIRCUIT

The transmitter was built for U.B.C. by Microwave Control Company, Farmingdale, New Jersey, U.S.A. A block diagram for the transmitter is shown in Figure 3.2.

The carrier frequency is generated by a crystal oscillator operating at a 120 MHz harmonic. The signal is then amplified by two NPN transistors, both operating class A (2N3866). Two more stages of amplification buffer the 120 MHz carrier.

The 120 MHz signal is fed to parallel x6 and x7 multipliers which yield 720 MHz signals for the local oscillator, and 840 MHz for the broadcast carrier. The 720 MHz signal passes through a bandpass filter to the local oscillator output jack. The 840 MHz carrier then drives two stages of tuned common base amplifiers. The first stage is gated by the modulator pulse which has been amplified from a TTL pulse provided by the external pulse generator. The second stage provides a maximum R. F. power of 20 watts.

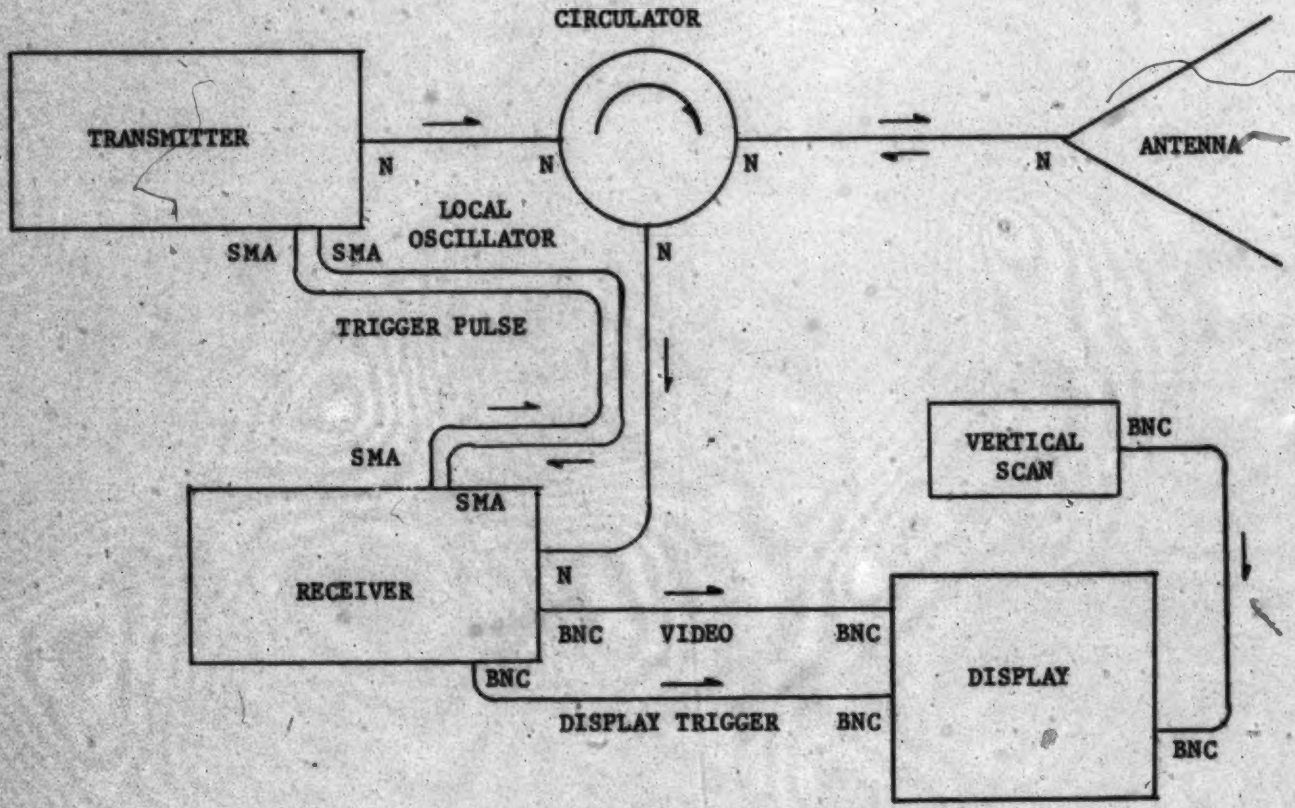
CIRCULATOR
TRANSMITTER
N
N
N
N
ANTENNA
LOCAL OSCILLATOR
SMA
SMA
N
TRIGGER PULSE
SMA
SMA
VERTICAL SCAN
BNC
RECEIVER
N
BNC
VIDEO
BNC
BNC
DISPLAY
DISPLAY TRIGGER
BNC
BNC

FIGURE 3.1: RADAR INTERCONNECTION DIAGRAM

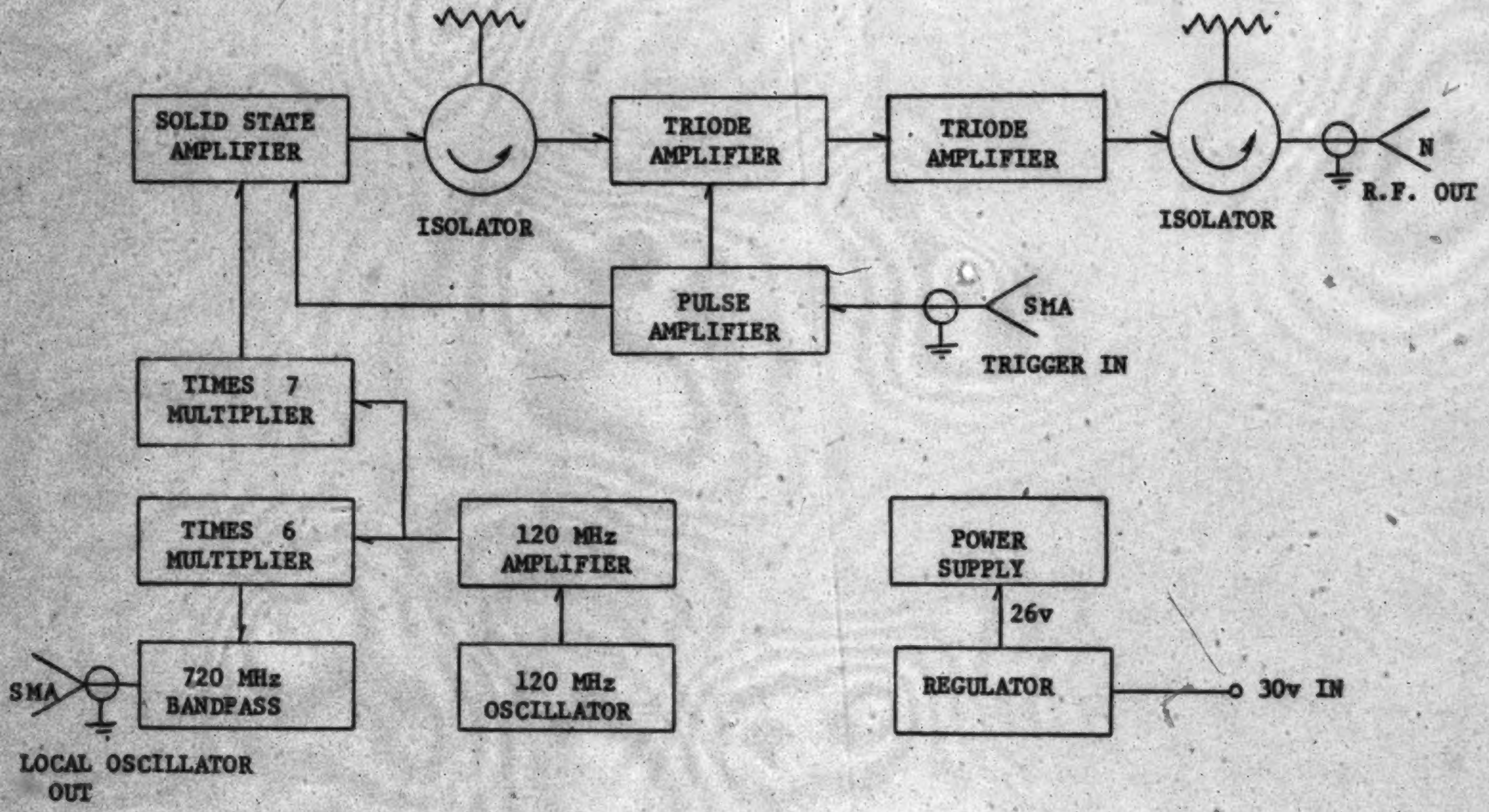
SOLID STATE AMPLIFIER
ISOLATOR
TRIODE AMPLIFIER
TRIODE AMPLIFIER
ISOLATOR
N
R.F. OUT
PULSE AMPLIFIER
SMA
TRIGGER IN
TIMES 7 MULTIPLIER
TIMES 6 MULTIPLIER
120 MHz AMPLIFIER
POWER SUPPLY
26v
SMA
720 MHz BANDPASS
120 MHz OSCILLATOR
REGULATOR
30v IN
LOCAL OSCILLATOR OUT

FIGURE 3.2: RADAR TRANSMITTER BLOCK DIAGRAM

The 20 watt R. F. power then passes through a 30 watt isolator to a triode amplifier/modulator, which is also gated by an amplified pulse from the external pulse generator. The high power modulated R. F. signal is then fed finally to a broad band triode power amplifier which delivers 4.1 kilowatts peak R. F. power through an isolator to the R. F. output jack.

Power for the transmitter is drawn from a 28 v - 30 v supply which is dropped and regulated to 26 v. All voltages used (up to 4 Kv) are derived from this 26 v regulated supply.

A digital timing circuit disables the high voltages for 1.5 minutes after turnon to allow for warmup. Internal sensing circuits provide for immediate shutdown should any subcircuit overload, for any reason. The shutdown circuit throws a circuit breaker which may be reset by applying a potential to a pin on a test jack provided.

3.2 RECEIVER/PULSE GENERATOR CIRCUIT

The receiver/pulse generator was designed and assembled at the University of British Columbia, Department of Geophysics. Figure 3.3 is a block diagram for the receiver/pulse generator.

The received R. F. signal passes through a diode switch which is enabled during the transmit pulse when the system is

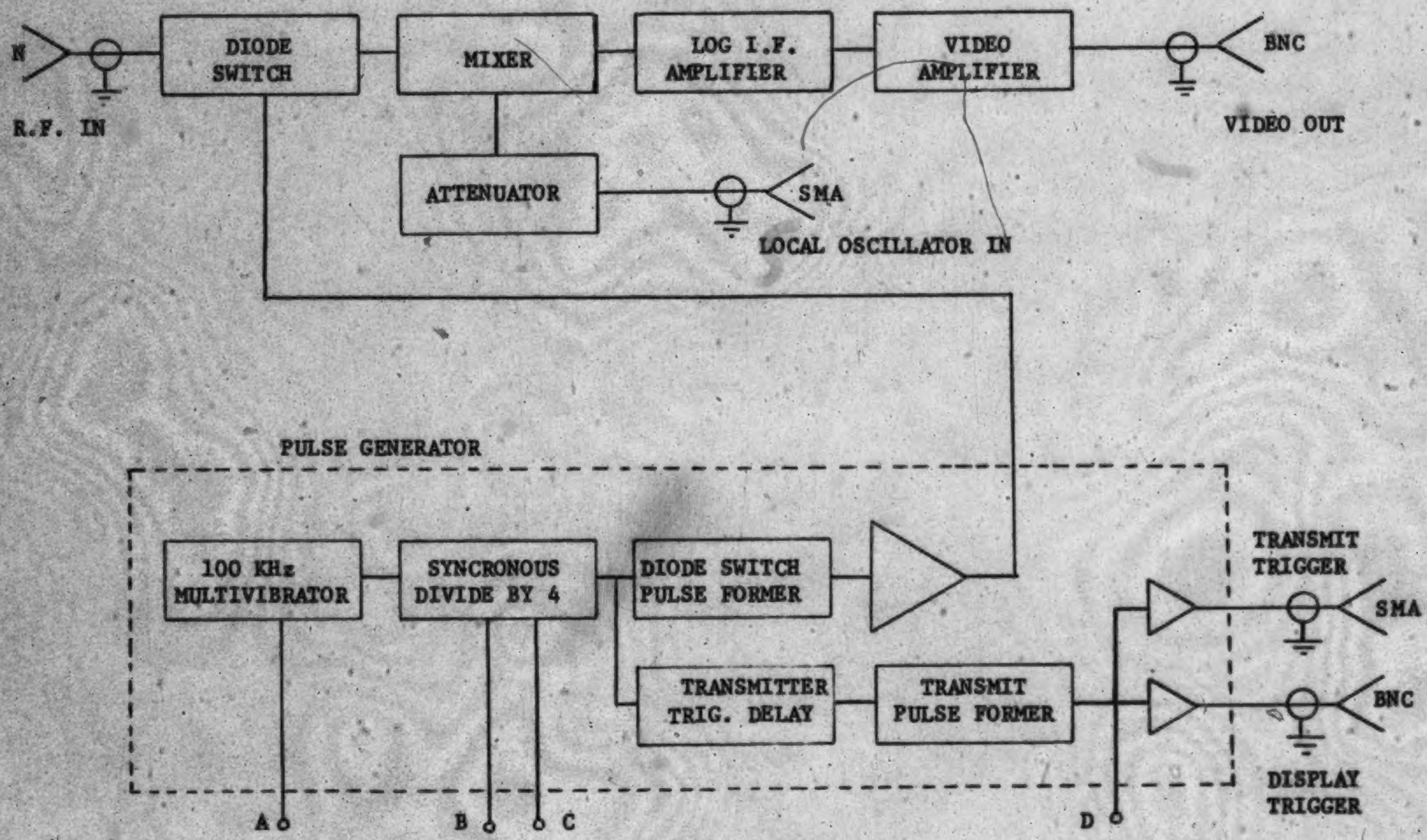
N
R.F. IN
DIODE SWITCH
MIXER
LOG I.F. AMPLIFIER
VIDEO AMPLIFIER
BNC
VIDEO OUT
ATTENUATOR
SMA
LOCAL OSCILLATOR IN
PULSE GENERATOR
100 KHz MULTIVIBRATOR
SYNCRONOUS DIVIDE BY 4
DIODE SWITCH PULSE FORMER
TRANSMITTER TRIG. DELAY
TRANSMIT PULSE FORMER
TRANSMIT TRIGGER
SMA
BNC
DISPLAY TRIGGER
A
B
C
D

FIGURE 3.3: RADAR RECEIVER BLOCK DIAGRAM

operated in the single antenna mode. The diode switch is enabled by an amplified pulse derived from the pulse generator.

The R. F. signal is then mixed down to the 120 MHz intermediate frequency, using the 720 MHz local oscillator provided in the transmitter. The local oscillator provides 22 dBm of R. F. power to the mixer. This is attenuated to 10 dBm. The mixer is a Mini Circuits Laboratory model MA-1 with a conversion loss of 8 dB.

The I. F. signal is then amplified through a logarithmic I. F. amplifier. The amplifier is an RHG model ICLT12040. It has a center frequency at 120 MHz, a 3 dB bandwidth of 40.1 MHz. It has a dynamic range of 97 dB and is linearly logarithmic (±1 dB) for 70 dB of its range. Its risetime is less than 20 ns; its noise figure is 10 dB. Its output voltage range is from 0.017 v at -90 dBm to 2.670 v at +7 dBm.

The detected video signal passes through one final stage of gain which adjusts amplitude and bias for display purposes.

The pulse generator provides trigger pulses to the transmitter, diode switch and oscilloscope display. It is capable of only a single repetition rate and pulse length. The repetition rate is determined by a 100 KHz TTL multivibrator. The 100 KHz clock pulse then passes through a divide-by-four TTL counter which provides the 25 KHz trigger pulse rate. The counter provides two bits of control information for a proposed digitizer. The 25 KHz pulse then drives two monostable TTL flipflops. One monostable pulse is amplified and enables the diode switch. The second monostable pulse provides a time delay between the diode switch enable pulse and a third monostable TTL flipflop. The third monostable vibrator is adjusted to have a pulse length of 70ns. This pulse provides the modulating signal to the transmitter and the trigger for the oscilloscope display. The length of the diode switch enable pulse is adjusted so that the switch and the transmitter disable simultaneously.

3.3 DISPLAY AND RECORDER

The initial display oscilloscope is a Tektronics model 475 oscilliscope with a Polaroid film pack. When operated using intensity modulation a ramp generator scans the vertical axis on the oscilloscope, which exposes one frame. The ramp generator consists of a variable clock pulse which drives a nine bit counter, which drives a digital to analog converter. Intensity and modulation amplitude are controlled by the video amplifier. A block diagram appears in Figure 3.4.

In addition it is hoped eventually to be able to digitize and record the complete radar record. The proposed digitizer will be capable of 1024 channels with 10 ns channel separation.the digitizer will sample 128 pulses at one time delay and average them. The time delay will then be incremented by 10 ns and the process will continue. The analog circuitry is based on a sample and hold amplifier with 175 MHz bandwidth designed by H. Baldis and J. Aazam-Zangeneih. The output will be eight bit parallel. A block diagram appears in Figure 3.5.

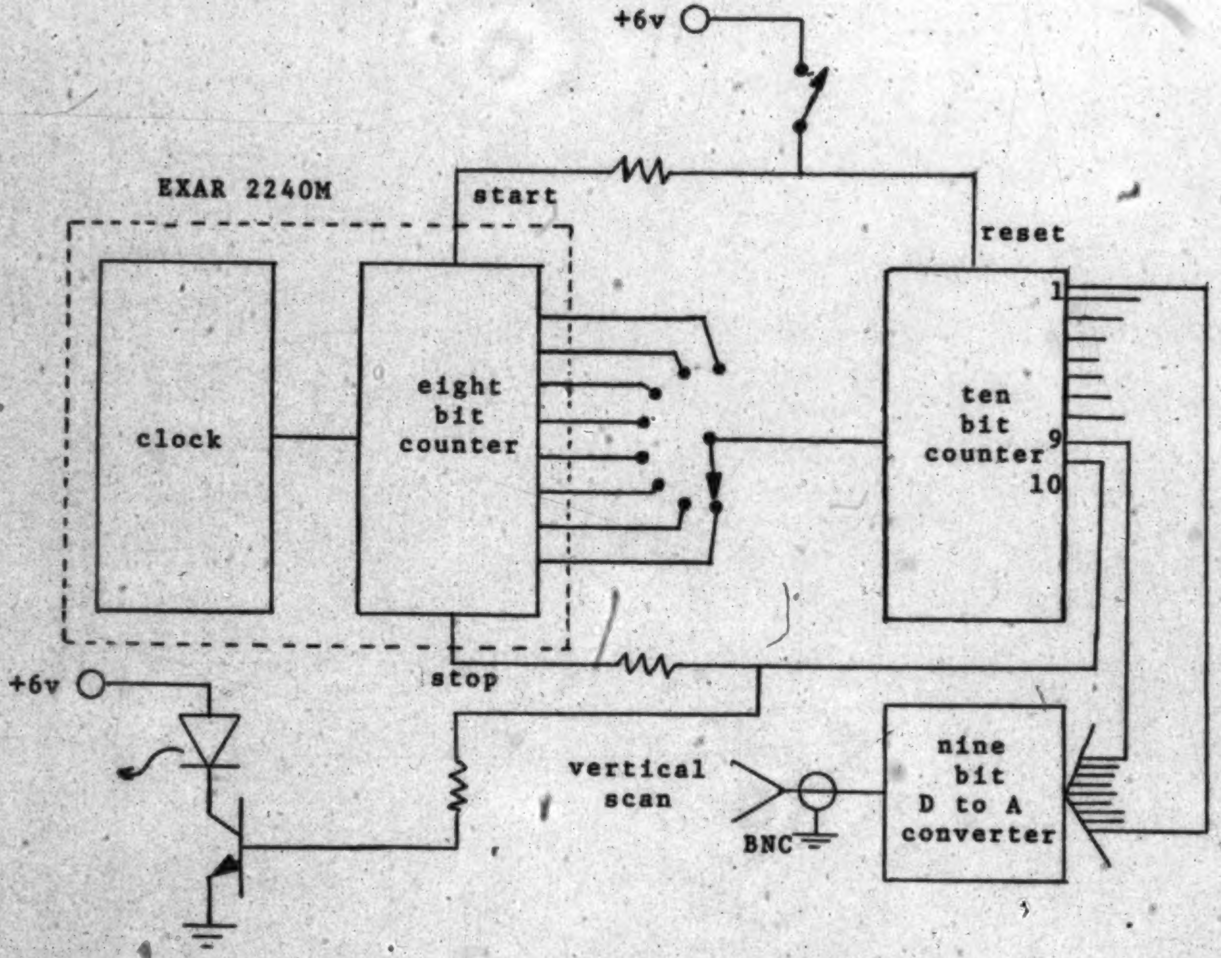
+6v
EXAR 2240M
start
reset
clock
eight
bit
counter
ten
bit
counter
1
9
10
+6v
stop
vertical
scan
BNC
nine
bit
D to A
converter

FIGURE 3.4: INTENSITY MODULATION RECORDING BLOCK DIAGRAM (vertical scan)

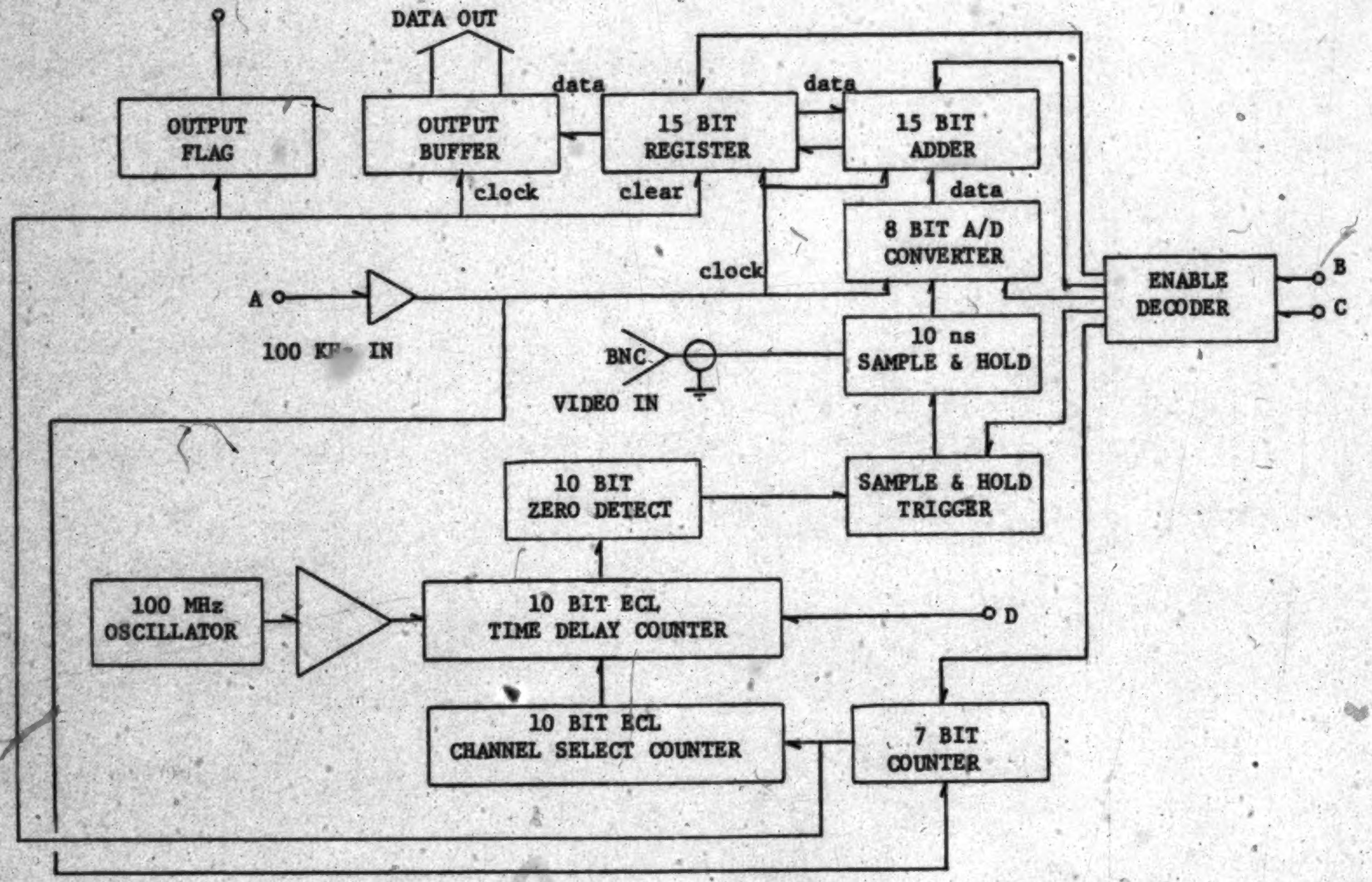
OUTPUT FLAG
DATA OUT
OUTPUT BUFFER
data
15 BIT REGISTER
data
15 BIT ADDER
clock
clear
data
8 BIT A/D CONVERTER
clock
ENABLE DECODER
B
C
A
100 KHz IN
BNC
VIDEO IN
10 ns SAMPLE & HOLD
10 BIT ZERO DETECT
SAMPLE & HOLD TRIGGER
100 MHz OSCILLATOR
10 BIT ECL TIME DELAY COUNTER
D
10 BIT ECL CHANNEL SELECT COUNTER
7 BIT COUNTER

FIGURE 3.5 RADAR DIGITIZER BLOCK DIAGRAM

CHAPTER 4: SYSTEM CAPABILITIES

4.1 SYSTEM PERFORMANCE

The maximum range of any radar system is a function of four parameters: antenna gain, frequency, medium attenuation and system performance. The latter is defined as the maximum r.m.s. transmitted power divided by the receiver sensitivity, thus system performance is a function of the transmitter and receiver parameters, but it is also possibly determined by antenna characteristics.

It is possible that there is sufficient transmitter leakage power, which may be available to the receiver, and could obscure otherwise usable echoes. In the present case this is a real consideration when a single antenna is used. If the ON/OFF transmitter ratio is only 100 dB and the circulator isolation is 25 dB, then system performance could be limited to their sum, 125 dB. Further, if the antenna is mismatched so that it has a reflection coefficient greater than -25 dB, then the system performance would be degraded still further. Any attempt to improve system performance by improving receiver sensitivity would be wasted.

This problem can be avoided by employing two antennae as with the SPRI Mk II sounder (Evans & Smith, 1969). It is relatively easy to produce antennae pairs with the required isolation, particularly if high gain antennae are used.

Another, possibly less expensive method is available for increasing isolation. Passive or active diode switches operated between the transmitter and circulator can increase the ON/OFF ratio by at least 40 dB. The only requirement on the switch is the ability to conduct the maximum transmitter power, with minimum loss. Switching speed is not critical as the switch need only be off for maximum range echoes, usually several microseconds after the transmitter pulse.

4.2 MAXIMUM RANGE AND RESOLUTION

In radio echo sounding in ice the bedrock has generally been modeled as a specular plane reflector with a reflection coefficient of -20 dB. This figure has been considered conservative (Davis, 1973). Deviations on this model have also been considered (Harrison, 1974). If the plane model is assumed then the maximum range is determined by

$$\frac{P_{\text{received}}}{P_{\text{transmitted}}} = \frac{G^2 \lambda^2 R}{64 \pi^2 r^2} 10^{-0.2Dr} \qquad (1)$$

where the left expression equals the inverse system performance, G is the free space antenna gain, λ is the free space wavelength, R is the bedrock reflectivity, D is the loss in $\mathrm{dBm^{-1}}$, and r is the range.

In cold ice, if the attenuation of the signal is 0.057 $\mathrm{dBm^{-1}}$, then the maximum range is 700 m, with the described apparatus, as stated in Chapter 2. In temperate ice the maximum range is only 210 m for a total attenuation of 0.2 dBm^{-1}. If total attenuation is 0.15 dBm^{-1} (Ragle et al, 1964), then the maximum range is 280 m. Improved gain due to refraction at the ice surface may improve the system performance by about 2 dB increasing the maximum range to 290 m in the last case.

If precision is defined as the time for echo power to rise 3 dB above local average power, then it follows that precision is a constant fraction of range. In the present case, precision is

$$\frac{18\text{ns} \cdot 88\text{m}/\mu\text{s}}{250\text{m}} = 0.63\% \qquad (4)$$

of range in temperate ice. In cold ice the precision is 0.25% of range. (Note: these figures are based upon the assumption that the plane reflector is sufficiently specular, that for the high gain antenna, the plane is effectively identical to a spherical reflector centered at the antenna with radius equal to the real range. The validity of the assumption is solely a function of the antenna gain and beamwidth. If fading patterns resulting from too broad a beam degrade the echo risetime, a deconvolution of the echo, if possible, using the transmitted pulse as a source function, will return this accuracy).

4

4.3 REFLECTIVITY OF LAYERS WITHIN A GLACIER

Harrison (1973) has shown that the reflection coefficient R, for random variations in permittivity vary with the pulse length in radians L, as

$$R \approx \{\frac{\Delta\varepsilon^2}{\varepsilon^2}\} L^2 e^{-2L^2} \tag{5}$$

where layer thickness is greater than the pulse length. $\frac{\Delta\varepsilon}{\varepsilon}$ is a step change of the relative permittivity with depth. Harrison has concluded that it is necessary to restrict oneself to the case where the layer thickness is much less than the pulse length. In this case

$$R = \frac{\pi^2 L_m^{\ 2}}{\lambda_m^{\ 2}} \{\frac{\Delta\varepsilon^2}{\varepsilon^2}\} \tag{6}$$

for single reflectors, and

$$R = \frac{\pi^3 p_m L_m}{\sqrt{8}\lambda_m^{\ 2}} \{\frac{\Delta\varepsilon^2}{\varepsilon^2}\} e^{-k_m^{\ 2} L_m^{\ 2}} \tag{7}$$

for multiple reflectors where L_m is the layer thickness or spacing, λ_m is the wavelength in ice, P_m is the pulse length in ice and k_m is the wave number in ice.

Harrison has also shown that there is a maximum reflectivity at $k_m l_m = 1/\sqrt{2}$ where

$$R_{max} = \frac{\pi}{16} p_m k_m \{\frac{\Delta\varepsilon^2}{\varepsilon^2}\} e^{-\frac{1}{2}} \tag{8}$$

In the present case, this reduces to

$$R_{max} = 0.119 \{\frac{\Delta\varepsilon^2}{\varepsilon^2}\} \tag{9}$$

at $L_m = 2.5$ cm. To obtain a power reflection coefficient of -70 dB in this case would require that

$$\frac{\Delta\varepsilon}{\varepsilon} = 10^{-3} \qquad (10)$$

It is clear that UHF radio echo sounders can be very sensitive to small variations in ε over centimeter ranges.

4.4 POLARIZATION

4.4.1 OPTICAL ACTIVITY

Optical activity is usually described as the tendency of transparent matter to rotate the E-vector of plane polarized electromagnetic radiation. The E-vector of any radiation traversing optically active matter will rotate either clockwise or counterclockwise when viewed from the radiation source.

With a radio echo sounder, plane polarized radiation enters a glacier at normal incidence. Any rotation due to optical activity in the ice during the first transit (to the bottom) should equal the rotation due to the return traverse. Since the rotation sense does not change, the total rotation should cancel. Hence radio echo sounding cannot detect optical activity.

4.4.2 DOUBLE REFRACTION

Double refraction (also known as birefringence) is defined as a difference in refractive index for radiation with E-vectors normal and parallel to a well defined crystal axis (Jenkins & White, 1957).

At visible wavelengths the ordinary and extraordinary indices of refraction in ice differ by 0.3%. In the ideal situation, with crystals having their optical axes parallel and horizontal, a 90° phase shift of the ordinary and extraordinary rays at 840 MHz could occur in only 16 meters of two way transit (it is necessary to assume that the ratio of refractive indices is constant with frequency above the relaxation spectrum). However this is excessively optimistic for two reasons. First, there is a tendency for the optical axes of ice crystals in glaciers to align vertically (Paterson, 1969). Secondly, and predominantly, nonuniformity in axis orientation causes double refraction to cancel. Consider an orthonormal base vector set, say vertical, in the direction of glacier flow, and horizontal and normal to glacier flow. By direction cosines the glacier can be divided into three equivalent thicknesses of ice with pure crystal axis orientations. The component with vertical axes does not exhibit double refraction and can be ignored. The equivalent thickness of ice available for affecting double refraction is equal to the difference of the other two components. Hence it is necessary to have a very strong prefered horizontal orientation to make double refraction visible. Sounding at frequencies of about 60 MHz, double refraction would require at least 120 m of ice to produce a 90° phase shift.

Jiracek (1965) reported that at South Pole Station, using a 30 MHz system, a bottom echo could not be received with antennae broadside and parallel. Maximum receiver power occurred when the antennae were perpendicular and horizontal. Jiracek interpreted this as a 90° rotation from the original transmitted pulse. "On the Skelton Glacier, bottom echo amplitude was practically independent of receiving antenna orientation in the horizontal plane." Jiracek interpreted this as a transformation of liner polarized radiation into near circular polarization by double refraction.

4.4.3 DETECTING DOUBLE REFRACTION

The orthonormal basis with one axis vertical, which maximizes the effective double refracting thickness defines the privileged directions in its two horizontal axes. These are the directions in which all of the transmitted power is either in the ordinary ray or the extraordinary ray. In these directions double refraction is not visible. However upon arrival at the bedrock the ideal reflector model fails by returning only a component fraction of polarized power instead of maintaining all polarization. The remaining reflected power is returned unpolarized. A receiver antenna based on dipoles, when rotated cannot distinguish between eliptically polarized radiation and combined linear and unpolarized radiation. All that is possible is a determination of the major axis of returned power. If this differs from the transmitted axis, then double refraction has been detected.

By rotating the transmitter antenna and repeating the procedure two transmitter antenna orientations should appear where no double refraction is evident, i.e. the major receiver power axis coincides with the transmitter power axis. At these positions an estimate for bedrock depolarization can be made. Once this is known it may be possible to estimate the amount of double refraction and hence draw a conclusion about the ice fabric.

4.4.4 FARADAY EFFECT

In many substances when plane-polarized radiation traverses in a direction parallel to an applied magnetic field, the plane of vibration is rotated. The amount of rotation θ is proportional to the field strength H, and to the distance traversed L. i.e.

$$\theta = VLH$$

where V, the Verdet constant is determined by the substance and the wavelength. For water V equals 0.0131 minutes $\text{Oersted}^{-1}\text{cm}^{-1}$ at the Sodium D lines. In the infrared V is the order of 10^{-3} minutes $\text{Oersted}^{-1}\text{cm}^{-1}$ (Jiracek, 1967).

When radiation is reflected back through the medium the field direction is effectively reversed, and the rotation due to the second traverse adds to the rotation due to the first traverse. This is unlike natural optical activity which cancels exactly. If Faraday rotation in ice due to the local magnetic field is detectable, it can be distinguished from double refraction by observing the average angular variation of receiver maximum from transmitter orientation, averaged over all transmitter directions.

Jiracek (1965) has considered the magnitude of the Faraday effect at the South Pole. He determined that rotation in the infra-red would be only 5°. Since the Verdet constant decreases with frequency (Jiracek, 1965) the effect should be negligibly small, even in the very thickest ice.

4.4.5 PHOTO-ELASTICITY

A transparent isotropic medium becomes optically anisotropic when subjected to mechanical stress. The privileged directions are along the directions of the principal stresses. Since photo-elasticity is optically identical to double refraction, the two effects cannot be distinguished.

It is unlikely that any information regarding the ice fabric can be determined a posteriori from information gathered by studying the effects of alpine or small valley glaciers upon polarized radio echo sounder radiation. All that may be possible is the detection of one or more of these effects.

4.4.6 DIGITAL RECORDS

A proposed digitizer having 8 bit resolution and 10 ns channel separation will be used to record the received envelope as provided by the output of the video amplifier. 10 ns channel separation yields a Nyquist frequency of 50 MHz so that no receiver power will alias into a lower frequency.

By deconvolving fading patterns using the transmitter pulse as a source function, and averaging over several records greater rangy accuracy should result and intermediate reflectors in the ice should become visible. Gross bottom roughness may be estimated by observing the spread in time of returned power from the bottom echo. Of particular interest would be the detection of fine interglacier structure near the bedrock.

4.5 CONCLUSION

This thesis has presented a basis for the design of a UHF radio echo sounder for the purpose of studying glaciers in mountainous terrain. Specific design parameters have been presented for a radio echo sounder to be built at the University of British Columbia. These parameters have been discussed and according to normal radio altimetry practices and engineering principles practical limits of the technique have been proposed. The design has followed as a basis a radio echo sounder built and operated by the Department of Energy, Mines and Resources, Ottawa, Canada, and Environment Canada, operating at 620 MHz. We suggest that UHF radio echo sounding will provide a highly mobile method of sounding the alpine and valley glaciers which have previously evaded successful study.

BIBLIOGRAPHY

Auty, R. P., *and* Cole, R. H. 1952. Dielectric properties of ice and solid D2O. *The Journal of Chemical Physics*, Vol. 20, No. 8, p. 1309-1314.

Bailey, J. T., Evans, S, *and* Robin, G. de Q. 1964. Radic echo sounding of polar ice sheets. *Nature*, Vol. 204, No. 4967, p. 420-421.

Baldis, H. A., *and* Aazam-Zanganeh, J. 1973. High speed single event sampler. *Reviews of Scientific Instruments*, Vol. 44, No. 6, p. 712-714.

Beckmann, P., *and* Spizzichino, A. 1963. The scattering of electromagnetic waves from rough surfaces. *Oxford, Pergamon Press*.

Berry, M. V. 1972. On deducing the form of surfaces from their diffracted echoes. *Journal of Physics A: General Physics*, Vol. 5, p. 272-291.

Berry, M. V. 1974. Theory of radio echoes from glacier beds. *Proceedings of the Symposium on Remote Sensing in Glaciology, Cambridge, September 1974*, in press.

Bleaney, B. I., *and* Bleaney, B. 1957. Electricity and magnetism. *Oxford, Clarendon Press*.

Bogorodskiy, V. V., *and* Fedorov, B. A. 1968. Radar sounding of glaciers. *Soviet Antarctic Expedition Information Bulletin*, Vol. 6, No. 65, p. 511-518 in AGU English translation.

Bogorodskiy, V. V., *and* Fedorov, B. A. 1970. Radar probing of Severnaya Zemlya Glaciers. *Arkticheskiy i Antarkticheskiy Nauchno-Issledovatel'skiy Institut, Trudy*, (Translated by Israel Program for Scientific Translations. Jerusalem, 1971, p. 1-11).

Bogorodskiy, V. V., Rudakov, V. N., *and* Tyul'pin, V. A. 1965. Electromagnetic probing of the Antarctic Ice Sheet. *Soviet Physics - Technical Physics*, Vol. 10, No. 6, p. 886-888.

Bogorodskiy, V. V., *and* Trepov, G. V. 1968. Radar measurements of the thickness of mountain glaciers. (Translated from *Zhurnal Tekhnicheskoy Fiziki*, Vol. 38, No. 8.) *Soviet Physics - Technical Physics*, Vol. 13, No. 8, 1969, p. 1135-36.

Calkin, P. E. 1971. Radio-echo sounding records from southern Victoria Land. *Antarctic Journal*, Vol. 7, p. 208-209.

Clarke, G. K. C., *and* Goodman, R. (In press) Radio echo sounding and ice temperature measurements in a surge type glacier. *Journal of Glaciology*.

Clough, J. W. 1973. Radio echo sounding: brine percolation layer. *Journal of Glaciology*, Vol. 12, No. 64, p. 141-143.

Clough, J. W., *and* Bentley, C. R. 1968. Measurements of electromagnetic wave velocity in the East Antarctic Ice Sheet. *IASH Publication 86*, p. 115-128.

Collin, R. E. 1966. Foundations for microwave engineering. *New York, McGraw - Hill*.

Cook, J. C. 1960. Proposed monocycle-pulse very-high-frequency radar for air-borne ice and snow measurement. *Transactions of the American Institute of Electrical Engineer*, Pt. 1, Vol. 79, p. 588-594.

Cumming, W. A. 1952. The dielectric properties of ice and snow at 3.2 centimeters. *Journal of Applied Physics*, Vol. 23, No. 7, p. 768-773.

Davis, J. L. 1973. The problem of depth sounding temperate glaciers. Unpublished, M.Sc Thesis, University of Cambridge.

Davis, J. L., Halliday, J. S., and Miller, K. J. 1972. Radio echo sounding of a valley glacier in East Greenland. Journal of Glaciology, Vol. 12, No. 64, p. 87-91.

Evans, S. 1963a. Radio techniques for the measurement of ice thickness. Polar Record, Vol. 11, No. 73, p. 406-410.

Evans, S. 1963b. International co-operative field experiments in glacier sounding. Polar Record, Vol. 11, No. 75, p. 725-726.

Evans, S. 1963c. Radio techniques for the measurement of ice thickness. Polar Record, Vol. 11, No. 75, p. 795.

Evans, S. 1965. Dielectric properties of ice and snow - a review. Journal of Glaciology, Vo. 5, No. 42, p. 773-786.

Evans, S. 1966. Progress report on radio echo sounding. Polar Record, Vol. 13, No. 85, p. 413-420.

Evans, S. 1969. Glacier sounding in the polar regions: a symposium. Geographical Journal, Vol. 135, Pt. 4, p. 547-563.

Evans, S., Drewry, D. J., and Robin, G. de Q. 1972. Radio echo sounding in Antarctica. Polar Record, Vol. 16, No. 101, p. 207-212.

Evans, S., and Robin, G. de Q. 1966. Glacier depth-sounding from the air. Nature, Vol. 210, No. 5039, p. 883-885.

Evans, S., *and* Smith, B. M. E. 1969. A radio echo equipment for sounding in polar ice sheets. *Journal of Scientific Instruments (Journal of Physics E)*, Series 2, Vol. 2, p. 131-[illegible].

Evans, S., *and* Smith, B. M. E. 1971. Radio echo exploration of the Antarctic Ice Sheet. *Polar Record*, Vol. 15, No, 96, p. 336-338.

Fitzgerald, W. J., *and* Paren, J. G. 1974. The dielectric properties of Antarctic ice. *Proceedings of the Symposium on Remote Sensing in Glaciology, Cambridge, September 1974*, in press.

Glen, J. W., *and* Paren, J. G. 1974. The electrical properties of snow and ice. *Proceedings of the Symposium on Remote Sensing in Glaciology, Cambridge, September 1974*, in press.

Goodman, R. H. 1970. Radio-echo sounding on temperate glaciers: a Canadian view. (Gudmandsen, P. ed.) *Proceedings of the International Meeting on Radioglaciology, Lyngby, May 1970*. Lyngby, Technical University of Denmark, Laboratory of Electromagnetic Theory, p. 135-146.

Goodman, R., *et al*. 1975. Radio soundings on Trapridge Glacier, Yukon Territory, Canada, by R. Goodman, G. K. C. Clarke, G. T. Jarvis, S. G. Collins, and R. Metcalfe. *Journal of Glaciology*, in press.

Gudmandsen, P. ed. 1970. Proceedings of the international meeting on radioglaciology, Lyngby, May 1970. *Laboratory of Electromagnetic Theory, the Technical University of Denmark, Lyngby*, R 86, 170 p.

Gudmandsen, P. 1972. Radio echo sounding of polar ice. *Laboratory of Electromagnetic Theory, the Technical University of Denmark, Lyngby*, D 170, 27 p.

Gudmandsen, P. 1973. Radioglaciology soundings at proposed drill sites. *Laboratory of Electromagnetic Theory, the Technical University of Denmark, Lyngby*, D 185, 20 p.

Harrison, C. H. 1970. Reconstruction of subglacial relief from radio echo sounding record. *Geophysics*, Vol. 35, No. 6, p. 1099-1115.

Harrison, C. H. 1971. Radio echo sounding: focusing effects in wavy strata. *Geophysical Journal of the Royal Astronomical Society*, Vol. 24, p. 383-400.

Harrison, C. H. 1972. Radio propagation effects in glaciers. Ph.D. thesis, Cambridge University.

Harrison, C. H. 1973. Radio echo sounding of horizontal layers in ice. *Journal of Glaciology*, Vol. 12, No. 66, p. 383-397.

Hattersley-Smith, G., Fuzesy, A., *and* Evans, S. 1969. Glacier depths in northern Ellesmere Island: airborn radio-echo soundings in 1966. *Ottawa, Defence Research Board, (Operation Hazen 36)*, 23 p.

Jasik, H. ed. 1931. Antenna engineering handbook. *New York, McGraw - Hill*.

Jenkins, A., *and* White, H. E. 1957. Fundamentals of optics. *New York, McGraw - Hill*.

Jiracek, G. R. 1965. Radio sounding of Antarctica ice. M.Sc. thesis, University of Wisconsin.

Jiracek, G. R. 1967. Radio sounding of Antarctic ice. *Research Report Series Number 67-1, The University of Wisconsin geophysical and Polar Research Center.*

Jiracek, G. R., *and* Bentley, C. R. 1965. Dielectric properties of ice at 30 Mc/sec. *Journal of Glaciology*, Vol. 6, No. 44, p. 319.

Kraus, J. D. 1940. The corner-reflector antenna. *Proceedings of the Institute of Radio Engineers*, Vol. 28, p. 513-519.

Kraus, J. D. 1950. Antennas. *New York, McGraw - Hill*.

Linlor, W. I. 1974. Electromagnetic reflection from multilayered models. *Proceedings of the Symposium on Remote Sensing in Glaciology, Cambridge, September 1974*, in press.

Longhurst, R. S. 1957. Geometrical and physical optics. *London, Longmans, Green and Co*.

Nye, J. F., Kyte, R. G., *and* Threlfall, D. C. 1972. Proposal for measuring the movement of a large ice sheet by observing radio echos. *Journal of Glaciology*, Vol. 11, No. 63, p. 319-325.

Oswald, G. K. A. 1974. Investigation of sub-ice bedrock characteristics. *Proceedings of the Symposium on Remote Sensing in Glaciology, Cambridge, September 1974*, in press.

Page, D. F., *and* Ramseier, R. O. 1974. Application of active radar techniques to the study of ice and snow. *Proceedings of the Symposium on Remote Sensing in Glaciology, Cambridge, September 1974*, in press.

Paren, J. G. 1970. Dielectric properties of ice. Ph.D. thesis, Darwin College, Cambridge.

Paterson, W. S. B. 1969. The Physics of Glaciers. *Oxford, Pergamon Press*.

Rinker, J. N. 1964. Radio echo sounding and strain rate measurement in the ice sheet of North-west Greenland; 1964. *Polar Record*, Vol. 12, No. 79, p. 403-405.

Ragle, R. H., *and others*. 1964. Ice core studies of Ward Hunt Ice Shelf, by R. H. Ragle, R. G. Blair and L. E. Persson. *Journal of Glaciology*, Vol. 5, No. 37, p. 39-59.

Robin, G. de Q., Evans, S., Drewry, D. J., Harrison, C. H., *and* Petrie, D. L. 1970. Radio echo sounding of the Antarctic Ice Sheet. *Antarctic Journal*, Vol. 6, p. 229-232.

Robin, G. de Q., Swithinbank, C. W. M., *and* Smith, B. M. E. 1968. Radio echo exploration of the Antarctic Ice Sheet. *IASH Publication 86*, p. 97-115.

Rossiter, J. R., *and others*. 1973. Radio interferometry depth sounding: part II - experimental results, by J. R. Rossiter, G. A. LaTorraca, A. A. Annan, D. W. Strangway and G. Simmons. *Geophysics*, Vol. 38, No. 3, p. 581-599.

Smith, B. M. E. 1971. Radio echo studies of glaciers. Ph.D. thesis, Cambridge University.

Smith B. M. E., *and* Evans, S. 1972. Radio echo sounding: absorption and scattering by water inclusions and ice lenses. *Journal of Glaciology*, Vol. 11, No. 61, p. 133-146.

Strangway, D. W., Simmons, G., LaTorraca, G., Watts, R., Bannister, L., Baker, R., Redman, J. D., *and* Rossiter, J. R. 1974. Radio-frequency interferometry - a new technique for studying glaciers. *Journal of Glaciolog*, Vol. 13, No. 67, p. 123-132.

Swithinbank, C. 1968. Radio echo sounding of Antarctic glaciers from light aircraft. *IASH Publication 79*, p. 405-414.

Swithinbank, C. W. M. 1972. Field work, Radio Echo Sounding by the British Antarctic Survey. *Polar Record*, Vol. 16, No. 102, p. 411-412.

Von Hippel, A. 1954. Dielectric materials and applications. *New York, Technology Press and Wiley*, p. 12, p. 301.

Waite, A. H. Jr. 1966. International experiments in glacier sounding, 1963 and 1964. *Canadian Journal of Earth Sciences*, Vol. 3, No. 6, paper 17, p. 887-892.

Waite, A. H., *and* Schmidt, S. J. 1962. Gross errors in height indication from pulsed radar altimeters operation over thick ice or snow. *Proceedings of the Institiute of Radio Engineers*, Vol. 50, No. 6, p. 1515-1520.

Walford, M. E. R. 1964. Radio echo sounding through an ice shelf. *Nature*, Vol. 204, No. 4956, p. 317-319.

Walford, M. E. R. 1965. Radio echo sounding of polar ice masses. Ph.D. thesis, Cambridge University.

Walford, M. E. R. 1968. Field measurements of dielectric absorption in Antarctic ice and snow at very high frequencies. *Journal of Glaciology*, Vol. 7, No. 49, p. 89-94.

Walford, M. E. R. 1972. Glacier movement measured with a radio echo technique. *Nature*, Vol. 239, p. 93-95.

Watts, R. D., England, A. W., Meier, M. F., *and* Vickers, R. S. 1974. Radio echo sounding of temperate glaciers at frequencies of 1 to 5 MHz. *Proceedings of the Symposium on Remote Sensing in Glaciology, Cambridge, September 1974*, in press.

Weber, J. R., *and* Andrieux, P. 1970. Radar sounding of the Penny Icecap, Baffin Island. *Journal of Glaciology*, Vol. 9, No. 55, p. 49-54.

APPENDIX

Some considerations on the selection and use of thermistors for the purpose of making absolute temperature measurements in snow or ice.

1 INTRODUCTION

In general, thermistors, when used as temperature measuring devices, are used singly or in pairs in some impedance net, that net being driven by some power supply, and also having an output, which is monitored by a detector. Frequently the thermistor is placed at the end of a transmission line (Fig. 1).

Errors in precision and accuracy enter from numerous sources: from the thermistor itself, from the power supply or its configuration, from the the detector, impedance net or transmission line.

The measurement of temperature can only be as good as the precision standard against which the thermistor was calibrated. If it has been assumed that the thermistor characteristic will fit a theoretical curve, then the accuracy can be no better than the quality of that fit.

Of necessity one must assume that a given thermistor will be stable over the long term, although it is known that this is not necessarily the case; environmental factors such as stress or moisture may affect a thermistor's behaviour, and over a period of time a thermistor's stucture may change. Preaging can reduce these effects, however they cannot be eliminated. If a thermistor is recoverable for recalibration after its period of use, it may be possible to monitor some of these effects.

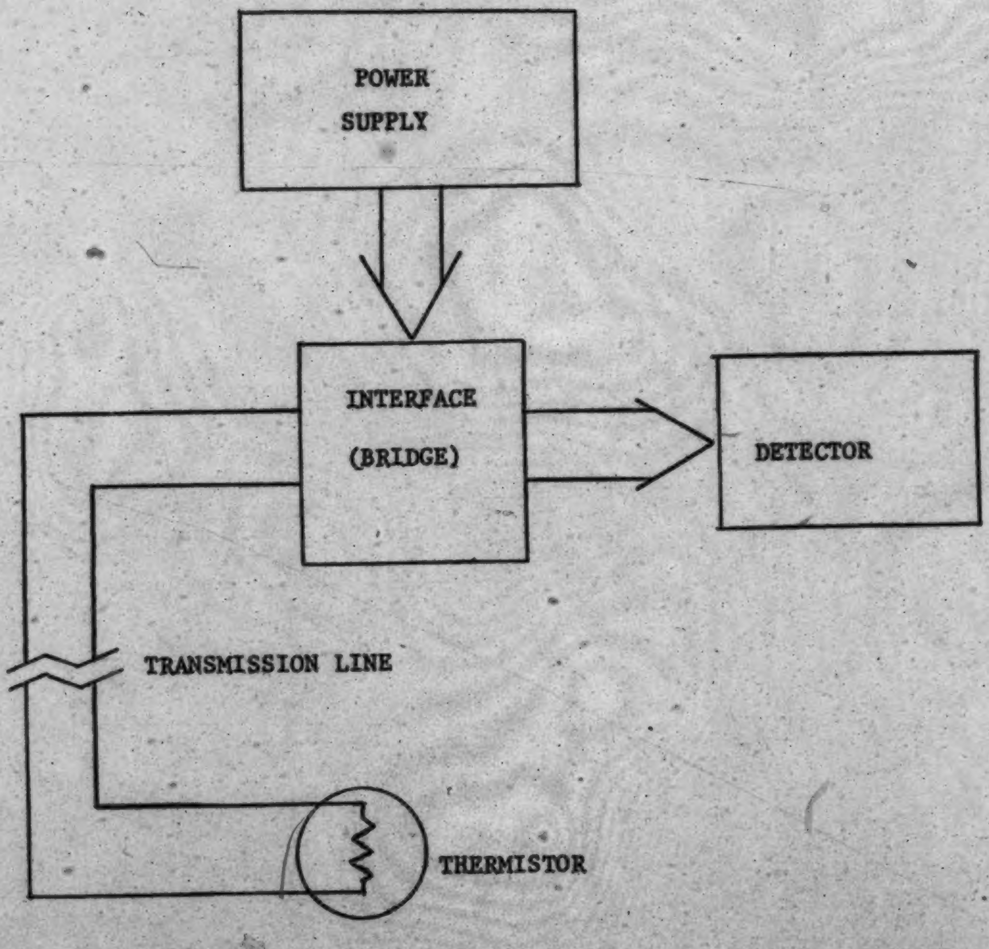
POWER SUPPLY
INTERFACE (BRIDGE)
DETECTOR
TRANSMISSION LINE
THERMISTOR

FIGURE 1: GENERALIZED BRIDGE

It is the intent of this paper to examine instrumental parameters, and to discuss how they may be used or determined, in order to optimize the precision with which the resistance of a given thermistor in a fixed situation, can be determined. These parameters include: thermistor self-heating, nominal thermistor resistance, transmission line resistance and reactance, impedance net or bridge configuration, type of bridge power supply, and quality of the detector. This examination applies equally to both calibration systems and field situations since both conditions can be completely described.

2 THERMISTOR CHARACTERISTICS

2.1 THERMISTOR SELF-HEATING

If we assume that a thermistor has spherical symmetry, and that the ambient temperature of the surrounding ice (or snow) is constant at T, then the steady state solution of the heat equation shows that the temperature of ice close to the thermistor can be no greater than

$$T + \frac{P}{4\pi k_{ice} r} \qquad (1)$$

where P is the power dissipated in the thermistor, K_{ice} is the thermal conductivity of ice (assumed to be constant with T) and r is the radius from the center of the thermistor. Let

$$\Delta T_{ice} = \frac{P}{4\pi k_{ice} r} \qquad (2)$$

and let $\Delta T + T$ be the temperature as indicated by the resistance of the thermistor. It follows that

$$\Delta T > \Delta T_{ice}\Big|_{min} = \frac{P}{4\pi k_{ice} r_{min}} \qquad (3)$$

where r_{min} is the radius of the ice closest to the thermistor; in effect the radius of the thermistor. Owing to the failure of our spherical approximation in (1) and to the great variety in structure and shape of thermistors, it shall be assumed here that the relation in (3) is an equality, where r_{min} must now be a typical radius.

Manufacturers of thermistors generally provide figures for their thermistors that indicate the ability of the device to dissipate power into the surrounding medium. This 'Dissipation Constant' which shall be called D_c, is specifically defined as the amount of power required to raise the temperature of the thermistor 1°C above the ambient temperature. More conveniently

$$D_c = \frac{dP}{d\Delta T} \qquad (4)$$

from (3), in ice

$$D_c = 4\pi k_{ice} r_{min} \qquad (5)$$

Equation (4) clearly depends on the environment of the thermistor. Manufacturer's figures are usually given for the thermistor in still air. In ice D_c is at least a factor of three greater [Fenwal D-1; Eq. (5)], and although increases in D_c will improve the measurement precision, a factor of three in D_c results in no more than 1.5dB improvement in precision. Hence for the examples used here, since D_c is generally difficult to measure or calculate, manufacturers' figures will be used.

2.2 THERMISTOR SELF-HEATING WITH WATER LAYER

If the temperature of the ice is sufficiently close to the melting point that before reaching steady state the temperature of the thermistor reaches the melting point a layer of water will form arround the thermistor. Since the thermal conductivity of water is much smaller than that of ice, the thermistor will tend to self-heat greatly. This effect has been demonstrated in attempts tc measure the thermal conductivity of ice by using a thermal drill cable as a line heater, and attempting to observe the logarithmic rise of temperature with time. If too much power is supplied to the cable a water layer forms before the logarithmic approximation becomes valid.

In another case, in temperate ice, the ice cannot conduct power away from the thermistor. The only available sink is in the ice melt, hence steady state will never be approached. However after sufficient time the ice/water boundary should be sufficiently distant and large, that it may be modelled as stationary. In this case

$$D_c = 4\pi k_{water} r_{min} \qquad (6)$$

Also if too much power is available, induced water currents may cause fluctuations in the thermistor temperature. Any system which must consider this case should be designed so that this effect is too small to be measurable.

2.3 THERMISTOR RESISTIVITY GRADIENT

Thermistors have negative thermal coefficients of resistivity, which shall be called R_T. For most thermistors

$$R_T = -0.05^0C^{-1} \qquad (7)$$

and this figure will be used in all of the examples in this paper.

2.4 TIME CONSTANTS

The 'time constant' of a thermistor, as defined by some manufacturers is the time required for a thermistor to change its temperature 63% of the amount of temperature change of a value impressed upon it in a step change [Fenwal EMC-5]. For a given thermistor this may vary from fractions of seconds to minutes [Fenwal D-1] as a function of environment.

For steady state temperature measurements a more useful time constant would be the time required for a thermistor to reach 63% of ΔT above T, from the initiation of power, but because of the effects of environment on Dc and hence ΔT, and also consideration of the fact that the two constants as defined here are probably closely related, the latter time constant is almost certainly indeterminable, especially when the thermistor would be deployed in a bore hole in ice.

The best that should be said about a thermistor being used to measure a steady state temperature is that the temperature it measures is between T and $T+\Delta T$, both as defined before. It is necessary then that the allowable error due to self-heating must be the full value of T, and that in most cases this will not be reduced.

3 BRIDGES AND BRIDGE POWER SUPPLY

3.1 POWER SUPPLY TYPES

In this paper only two kinds of power supply will be considered. They are first a D.C. supply, and secondly an A.C. supply of angular frequency ω . Further in this paper they will be shown to be both optimal when compared to pulsed supplies.

3.2 BRIDGE TYPES

The simplest type of resistance measuring device consists of a current source driving the unknown resistance. A voltmeter then measures the voltage drop accross the resistance (Fig. 2A). A measure of the signal available is dV/dR. In this case

$$\frac{dV}{dR} = i \qquad (8)$$

Thermal noise voltage is proportional to $\sqrt{R}$ provided we assume that the thermistor is an ideal Johnson noise generator. Signal to noise ratio is thus proportional to $i/\sqrt{R}$.

All analog ohmmeters and digital ohmmeters work in this fashion. The difficulties involved in taking this approach is that with analog meters, they rarely have enough dynamic range or precision to be useful, and with digital meters long term linearity and short term thermal stability are generally not good enough so that overall accuracy approaches the resolving capability of the instrument. This is particulary the case when different instruments are used for calibration and field measurements.

Null detectors have the advantage that they do not require the dynamic range or linearity of the 'ohmmeter' type of instrument. However, they may still be thermally

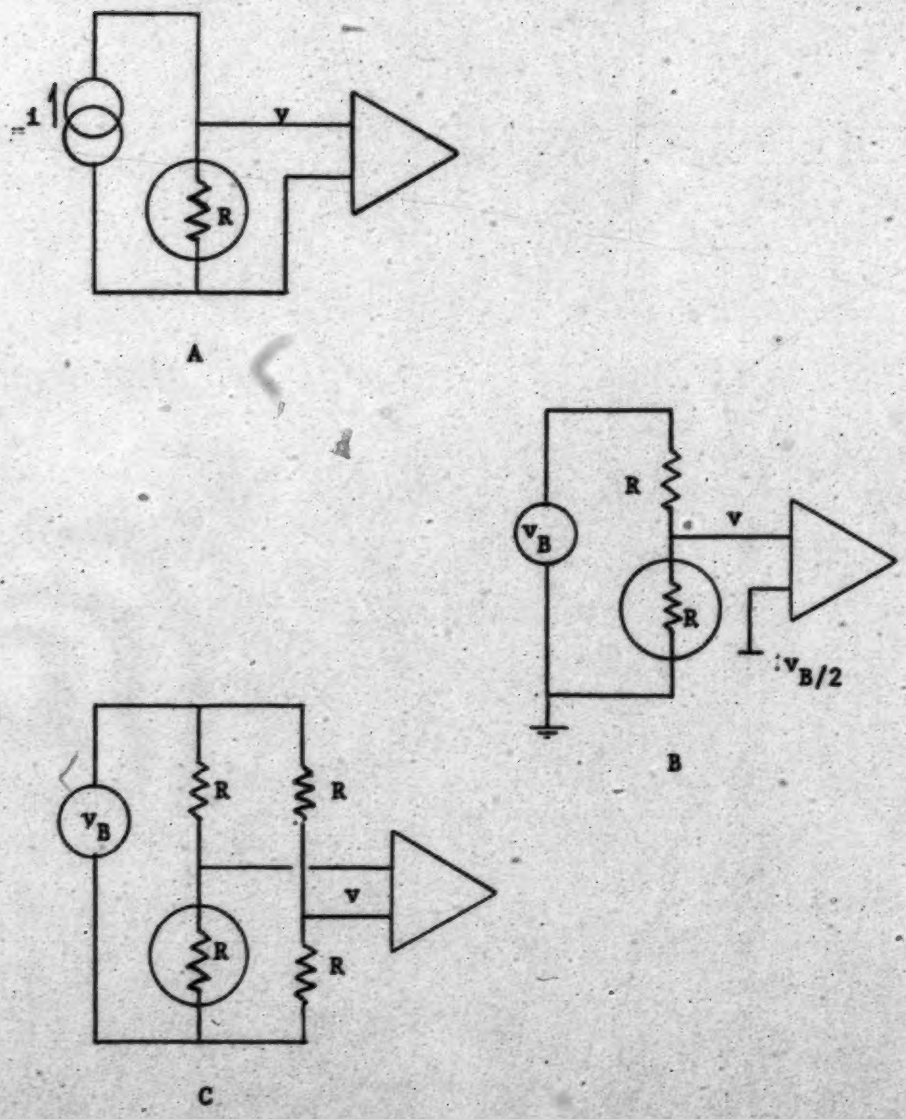
i
v
R
A
R
v
v_B
R
$v_{B/2}$
B
v_B
R
R
v
R
R
C

FIGURE 2: BRIDGE CONFIGURATIONS

sensitive, and they cannot be used for 'instant' measurements. This is a problem if continuous measurements in time over a large temperature range are required. For making single measurements of steady state temperatures, null detectors are well suited. Figures 2B and 2C show two possible configurations. The chief difficulty in implementing a system generalized by the type in Figure 2B lies in providing an accurate low impedance voltage reference $v_B/2$ exactly half of the primary bridge supply (In all cases v_B refers to the R.M.S. Voltage). Figure 2C represents a Wheatstone bridge with the four arms equal.

In Figure 2B

$$\frac{dV}{dR} = \frac{V_B}{4R} \tag{9}$$

and noise voltage is $\sqrt{2}$ times smaller than in case A. Signal to noise voltage ratio is then proportional to

$$\frac{V_B}{\sqrt{8R^3}}$$

If power dissipated in the thermistor is the same in both cases

$$i^2R = \frac{V_B^2}{4R} \tag{10}$$

and signal to noise ratios may be compared. It follows that S/N voltage ratio for case A is $\sqrt{2}$ times greater than for case B, and is two times greater than for case C (Fig. 2C).

Difficulties in constructing relatively noiseless current and voltage sources would likely counter the advantages of case A or B over case C. For this reason, and for ease in calculations, case C will continue to be used.

3.3 BRIDGE AND DETECTOR RESOLUTION

Let ΔT^* be the desired temperature resolution. Then

$$\frac{\Delta R}{R} = \Delta T^* R_T \tag{11}$$

where ΔR is the necessary resolution in terms of resistance. From (9) and (11)

$$\frac{V_B}{\Delta V} = \frac{4}{\Delta T^* R_T} \tag{12}$$

where ΔV is the required voltage resolution of the detector.

Johnson noise power from the bridge is ideally

$$P_n = \frac{V_n^{\,2}}{R} = 4kTB \tag{13}$$

where V_n is noise voltage, k is Boltzmann's constant, T is in degrees Kelvin, and B is the bandwidth of the detector. A convenient measure of the quality of the detector may be defined as

$$S_n = \frac{\Delta V}{V_n} = \text{noise figure} \tag{14}$$

where ΔV now represents the detector's best resolving ability. Recall from (10) that

$$P = \frac{V_B^{\,2}}{4R}$$

From (10), (12), (13), and (14)

$$\Delta T^* = \left(\frac{16 S_n^{\,2} kTB}{P R_T^{\,2}}\right)^{1/2} \tag{15}$$

But from (4)

$$P = \Delta T D_c \tag{16}$$

A minimum of the sum of ΔT and ΔT^* occurs at

$$\frac{\Delta T^*}{2} = \Delta T \tag{17}$$

It follows that

$$\Delta T = \left(\frac{4 S_n^{\,2} kTB}{D_c R_T^{\,2}}\right)^{1/3} \tag{18}$$

$$\Delta T^* = \left(\frac{32 S_n^{\,2} kTB}{D_c R_T^{\,2}}\right)^{1/3} \tag{19}$$

$$\Delta T + \Delta T^* = \left(\frac{108 S_n^{\,2} kTB}{D_c R_T^{\,2}}\right)^{1/3} \tag{20}$$

Equations (18), (19) and (20) are useful for determining the optimum resolution of any system as the parameters approach the ideal. More realistically it would be convenient to have an expression for the optimum in terms of the detector resolution ΔV. From (13), (14), (18), (19) and (20)

$$\Delta T = \left(\frac{\Delta V^2}{RD_cR_T{}^2}\right)^{1/3} \qquad (21)$$

$$\Delta T^* = \left(\frac{8\Delta V^2}{RD_cR_T{}^2}\right)^{1/3} \qquad (22)$$

$$\Delta T + \Delta T^* = \left(\frac{27\Delta V^2}{RD_cR_T{}^2}\right)^{1/3} \qquad (23)$$

From (21), (22) and (23) detector parameters and power levels may be optimized, and overall accuracies known. Consider for example a thermistor with $D_C = 1mW^oC^{-1}$ which shall be operated at 10KΩ. Suppose our detector has an input noise voltage of 1μV. Then

$$\Delta T + \Delta T^* = 0.001^oC$$

Here signal power has been assumed to be equal to noise power. Generally it would be desirable to have signal tc noise ratios of at least 10dB. Then

$$\Delta T + \Delta T^* = 0.0023^oC$$

3.4 D.C. BRIDGES

If a D.C bridge is used with a good detector [eg. ANALOG DEVICES chopper amp. Model 261K] it would have input noise on the order of $1\mu V$ P-P with a bandwidth to 10Hz. Since a reasonable response time is desirable, a bandwidth of 5 Hz is minimal. Input noise voltage drift of $0.1\mu V {}^{\circ}C^{-1}$ would boost effective input voltage noise to about $3.5\mu V$. This would boost a usable ΔV to $12\mu V$, and in our example

$$\Delta T + \Delta T^* = 0.0054^0C$$

This may be considered a practical limiting accuracy for a thermistor with $D_c = 1\ mW {}^{\circ}C^{-1}$ and $R = 10K\Omega$, when driven by a D.C. system.

Other difficulties involved in using a D.C. system arise from thermal voltage offsets, and from the proximity of 50 Hz or 60 Hz sources. The first may be helped by selecting a chopper stabilized detector or similar detector designed for thermal immunity. The second, which may be large enough to obscure measurements in spite of a sharp roll off should be helped by using good shielding and grounding (the most likely mechanism would be that the transmission line, acting like an antenna, would provide sufficient common mode signal to overload the detector input).

3.5 A.C. BRIDGES

It is possible to get amplifiers which operate at audio frequencies, that have considerably less input noise voltage per unit bandwidth than D.C. amplifiers. Detectors, either phase-locked, or simple, are easily designed. Bandwidths may be limited to less than 100 Hz, which will keep input noise voltage well below the best available D.C. detectors. For systems where extremely high precision is necessary, the designer may consider using an A.C. voltage source to feed his bridge.

However, new design problems accompany the choice of an A.C. source. The operating frequency should be kept as low as possible. The reason is twofold: first, since a low bandwidth is desirable, a low center frequency would minimize the need for a large Q; second and predominant, the effects of stray reactance in the bridge, and particularly in the transmission line to the thermistor would be minimized. Below 100 Hz flicker noise predominates and all the difficulties of D.C. bridges ensue.

3.6 OPTIMUM BRIDGE SUPPLIES

It is possible to use a pulsed power supply or some other form of intermittent supply. However in no case can one improve on either a pure D.C. or pure sine wave source if one considers the signal to noise ratio. This can be shown as follows. Since all measurements must be of finite duration we can assume that the power supply pattern repeats regularly. Consider its Fourier decomposition. The maximum signal to noise ratio occurs when all the signal power is confined to the minimum bandwidth; i.e. in one component. Any attempt of spreading the signal power among more than one component necessarily increases the required bandwidth of the detector and thus increases noise. Hence a single component, sine wave or pure D.C. is optimal.

4 TRANSMISSION LINE EFFECTS

4.1 TRANSMISSION LINE RESISTANCE

Presumably it is possible to determine the resistance of the transmission line being used, or at least get an estimate well within the required accuracy. This may then be corrected for when determining the actual thermistor resistance. If a three or four wire transmission line is used, the problem can be eliminated entirely.

4.2 TRANSMISSION LINE REACTANCE

In an A.C. bridge, it is desirable to know what the maximum transmission line capacitance C is which will still permit a null of amplitude V. If C is sufficiently small, then its effect is to phase shift the current, amplitude changes being second order. The constraint on C is

$$\omega RC < \frac{\Delta V}{V_B} \qquad (24)$$

If the detector is phase-locked then

$$R_{observed} = \left|\frac{1}{j\omega C}//R_{actual}\right| \qquad (25)$$

To a first approximation

$$\Delta R = R_{actual} - R_{observed} \approx \frac{R}{2}(\omega RC)^2 \qquad (26)$$

provided the transmission line is short (this error will usually be sufficiently small that an estimate of C will yield a correction ΔR of sufficient accuracy).

5 EVALUATION OF AVAILABLE SYSTEMS (DMM.S)

On the basis of (16) and the relation of ΔT^* to P (from (13) (14) and (15))

$$\Delta T^* = \frac{2\Delta V}{R_T\sqrt{PR}} \qquad (27)$$

It is possible to evaluate and compare measurement systems for a given R and D_c.

The following digital multimeters have been evaluated as thermistor measurement systems with respect to thermistor selfheating, displayed precision, guaranteed accuracy, each when used with a FENWAL GB34P2 thermistor - $10K < R < 15K$, $D_c = 1mW°C^{-1}$.

FLUKE MODEL 8100A

FLUKE MODEL 8000A

DANAMETER 2000

DATA PRECISION 245

SYSTRON DONNER 7205

SYSTRON DONNER 7050

SYSTRON DONNER 7005

TABLE 1: DIGITAL MULTIMETERS

Table Two lists pertinent data.

CONCLUSION

Present technology can easily yield a device for measuring thermistor resistances within 0.01°C, however the value of achieving this resolution of absolute temperature measurements can be questioned.

In deep boreholes, where the thermistor resistances are used to infer both absolute temperatures and temperature gradients, the thermistors are not recoverable and long term stability limits the accuracy possibly to only 0.4°C (Muller & Stolton, 1953) although 0.08°C is more common [Fenwal- TI-1] and0.02°C is possible (Beck, 1956).

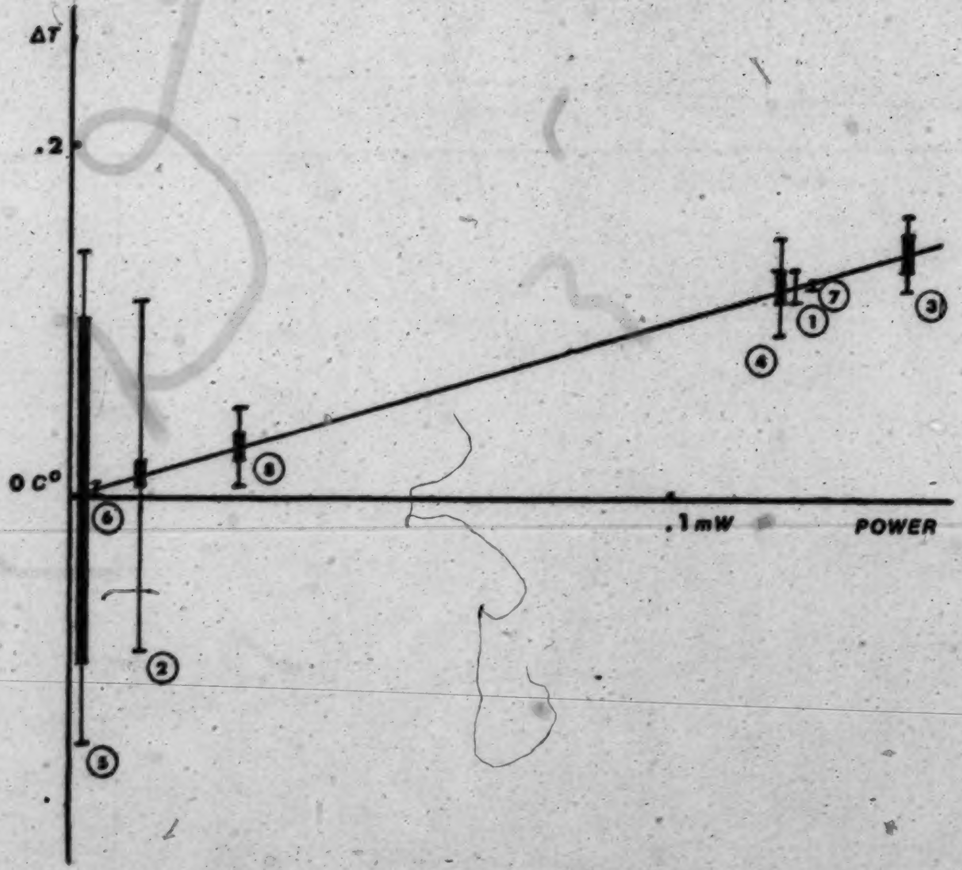

Errors in Temperature Measurement vs. Power to a FENWAL GB34P2 Thermistor, for Seven Digital Voltmeters

The diagonal line represents thermistor self-heating. The thick error bars represent the meter resolution. The thin error bars represent the meter accuracy. The numbers in circles indicate the points plotted from Table 2.

FIGURE 3: DIGITAL MULTIMETER ERRORS

UNIT	RANGE	POWER	ΔT	$\Delta T^*(1)$	$\Delta T^*(2)$	
FLUKE 8100A						
	12KΩ	120μW	0.12°C	0.002°C	0.02°C	①
	120 KΩ	13μW	0.013°C	0.02°C	0.2°C	②
DATA PRECISION 245						
	20KΩ	1.3mW	1.3°C	0.002°C	0.1°C	
DANAMETER 2000						
	20KΩ	140μW	0.14°C	0.02°C	0.04°C	③
FLUKE 8000A						
	20KΩ	120μW	0.12°C	0.02°C	0.06°C	④
SYSTRON DONNER 7050						
	150KΩ	1.2μW	0.001°C	0.2°C	0.28°C	⑤
SYSTRON DONNER 7205						
	130KΩ	1.2μW	0.001°C	0.002°C	0.01°C	⑥
	13KΩ	120μW	0.12°C	0.0002°C	0.001°C	⑦
SYSTRON DONNER 7005						
	130KΩ	30μW	0.03°C	0.02°C	0.04°C	⑧
	13KΩ	3mW	3°C	0.002°C	0.004°C	

TABLE 2: DIGITAL MULTIMETER ERRORS

Data lines followed by numbers in circles are graphed for comparison in Figure 3. $\Delta T^*(1)$ is the resolution determined by the number of available digits. $\Delta T^*(2)$ is the effective guaranteed accuracy of the meter.

In shallow experiments such as snow pack studies, or permafrost detection, fine temperature resolution is not required since in one case the temperature variations are gross and nonlinear, and in the latter the experimenter generally wishes only to detect subfreezing temperatures, not to estimate them.

The greatest value in achieving fine resolution of thermistor resistances lies first in thermistor calibrations (it is possible to achieve 0.03% accuracy easily and rapidly) and in experiments where temperature transients are measured.

Thermistor measurement technique is an important consideration in any temperature measurement system where optimum accuracy is required. Errors due to thermistor stability, reference temperatures, and measurement are comparable in magnitude. As the quality of thermistors and thermometers improve, so should the techniques of thermistor use.

BIBLIOGRAPHY

Baxandall, P. J. 1968. Noise in transistor circuits, part 1. *Wireless World*, November 1968, p. 388-92.

Baxandall, P. J. 1968. Noise in transistor circuits, part 2. *Wireless World*, December 1968, p. 454-59.

Beck, A. 1956. The stability of thermistors. *Journal of Scientific Instruments*, Vol. 33, p. 16-18.

Beck, A. E. 1963. Lightweight borehole temperature measuring equipment for resistance thermometers. *Journal of Scientific Instruments*, Vols . 40, p. 452-4.

Bosson, G., Gutmann, F., *and* Simmons, L. M. 1950. A relationship between resistance and temperature of thermistors. *Journal of Applied Physics*, Vol. 32, No. [illegible] p. 1267-68.

Carslaw, H. S., *and* Jaeger, J. C. 1959. Conduction of heat in solids, second edition. *Oxford Clarendon Press*.

Clarke, G. K. C., *and* Goodman, R. (In press) Radio echo sounding and ice temperature measurements in a surge type glacier. *Journal of Glaciology*.

Classen, D. F., *and* Clarke, G. K. C. 1972. Thermal drilling and ice temperature measurements in the Rusty Glacier (in Bushnell, V. C. *and* Ragle, R. H. Ed. Icefield Ranges Research Project. Scientific Results. Vol. 3. New York, American Geographical Society; Montreal Arctic Institute of North America, p. 103-16).

Doucet, Y., *and* Guignard, J. P. 1952. Essai d'interpretation de la loi donnant la resistance des "thermistors" en fonction de la temperature. *Academie des Sciences-Comptes Rendus*, Vol. 234, No. 19, p. 1856-58.

Garfinkel, C. L. 1974. How to match readouts to temperature transducers. Electronics, Vol. 47, No. 24, p. 117-123.

Greenhill, E. B., and Whitehead, J. R. 1949. An apparatus for measuring small temperature changes in liquids. Journal of Scientific Instruments, Vol. 26, p. 92-95.

Harrison, W. D. 1972. Temperature of a temperate glacier. Journal of Glaciology, Vol. 11, No. 61, p. 15-29.

Jarvis, G. T. (unpublished) Thermal studies related to surging glaciers. (M.Sc. Thesis, U.B.C. 1973).

Jarvis, G. T., and Clarke, G. K. C. (unpublished) The thermal regime of Trapridge Glacier and its relevance to glacier surging.

Jessop, A. M. 1964. A lead-compensated thermistor probe. Journal of Scientific Instruments, Vol. 41, p. 503-504.

Jessop, A. M., and Judge, A. S. 1974. Temperature measurement in boreholes for the mining industry. Division of Seismology, Earth Physics Branch, Department of Energy, Mines and Resources, Ottawa, Canada.

Letzter, S., and Webster, N. 1970. Noise in amplifiers. IEEE Spectrum, August 1970, p. 67-75.

Lliboutry, L. 1971. Permeability, brine content, and temperature of temperate ice. Journal of Glaciology, Vol. 10, No. 58, p. 15-29.

Misener, A. D., and Thompson, L. G. D. 1952. The pressure coefficient of resistance of thermistors. Canadian Journal of Technology, Vol. 30, p. 89-94.

Muller, R. H., and Stolton, H. J. 1953. Use of thermistors in precise measurements of small temperature differences. Analytical Chemistry, Vol. 25, No. 7, p. 1103-06.

Paterson, S. B. 1972. Temperature distribution in the upper layers of the ablation area of Athabasca Glacier, Alberta, Canada. *Journal of Glaciology*, Vol. 11, No. 61, p. 31-41.

Staley, R. C. 1952. Performance characteristics of Sanborn rod thermistors. *American Meteorological Society Bulletin*, Vol. 32, No. 2, p. 67-72.

Stuart, J. R. 1973. An approach to audio amplifier design, part 1. *Wireless World*, August 1973, p. 387-91.

Stuart, J. R. 1973. An approach to audio amplifier design, part 2. *Wireless World*, September 1973, p. 439-46.

Stuart, J. R. 1973. An approach to audio amplifier design, part 3. *Wireless World*, October 1973, p. 491-94.

Technical Note: Thermistor Manual. FENWAL ELECTRONICS, INC., EMC-5.

Technical Note: [Thermistor] Stability and Reliability Characteristics. FENWAL ELECTRONICS, INC., TD-1.

Technical Note: Considerations in the testing of thermistors. FENWAL ELECTRONICS, INC., TD-2, EM-34/ Revision 2.

Biographical Information

NAME: BRIAN BARRY NAROD

PLACE AND DATE OF BIRTH: SEATTLE, WASHINGTON, U.S.A.
October 31, 1949

EDUCATION (Colleges and Universities attended, dates, degrees)

UNIVERSITY OF B.C. 1971-75 M.Sc.
1966-70 B.Sc.

UNIVERSITÉ DE MONTRÉAL 1965

POSITIONS HELD:

PUBLICATIONS:

"BRIDGE OPTIMIZATION FOR THERMISTORS"
JOURNAL of GLACIOLOGY (IN PRESS)

AWARDS:

GOVERNMENT OF QUEBEC SCHOLARSHIP FOR
STUDY OF MATHEMATICS - 1965

This form is to be completed by candidates for the Master's or higher degree and submitted to the University Library Special Collections Division with the thesis.

DE-1 BP 74-4485